Natural Resources Canada | Ressources naturelles Canada

GEOLOGICAL SURVEY OF CANADA
OPEN FILE 8736

Understanding plateau landslides: current research in the Thompson River valley, Interior Plateau, British Columbia (2013-2020)

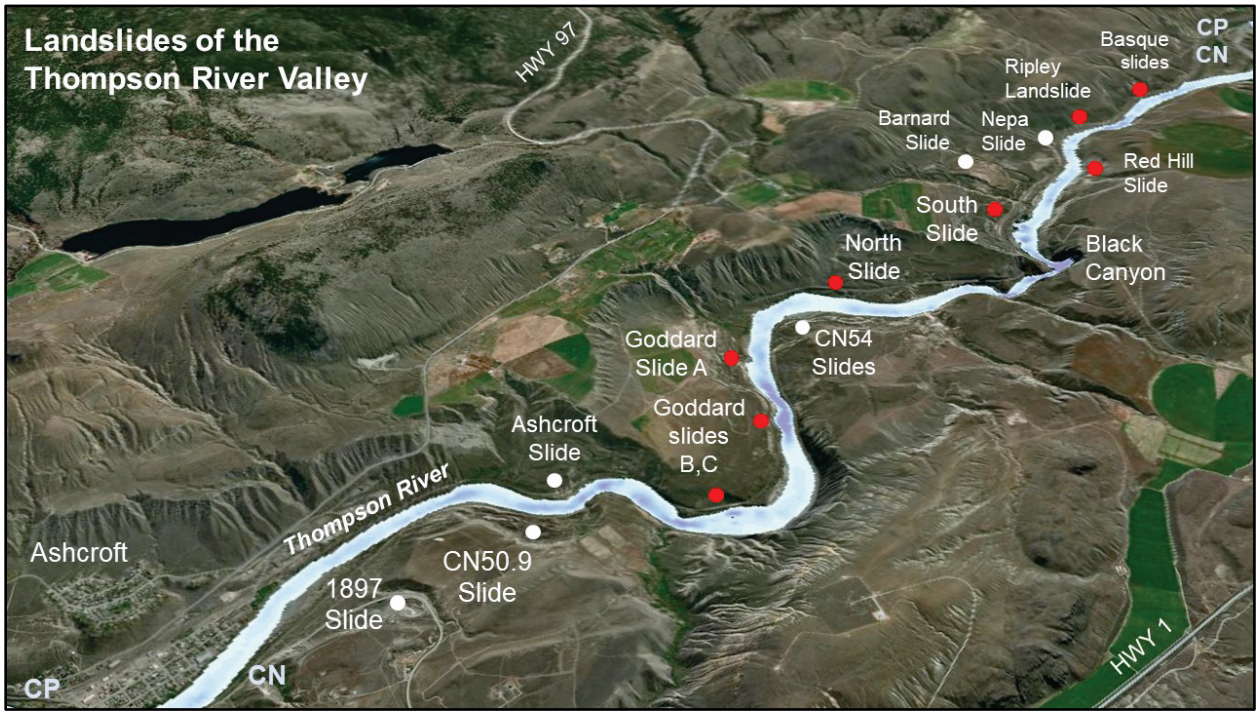

D. Huntley, P. Bobrowsky, D. Rotheram-Clarke, R. MacLeod, R. Cocking, and J. Joseph

2020

Canada

GEOLOGICAL SURVEY OF CANADA
OPEN FILE 8736

Understanding plateau landslides: current research in the Thompson River valley, Interior Plateau, British Columbia (2013-2020)

D. Huntley, P. Bobrowsky, D. Rotheram-Clarke, R. MacLeod, R. Cocking, and J. Joseph

2020

Permanent link: https://doi.org/10.4095/326830

This publication is available for free download through GEOSCAN (https://geoscan.nrcan.gc.ca/).

Recommended citation

Huntley, D., Bobrowsky, P., Rotheram-Clarke, D., MacLeod, R., Cocking, R., and Joseph, J. 2020. Understanding plateau landslides: current research in the Thompson River valley, Interior Plateau, British Columbia (2013-2020); Geological Survey of Canada, Open File 8736, 58 pages. https://doi.org/10.4095/326830

Publications in this series have not been edited; they are released as submitted by the author.

Understanding Plateau landslides: current research in the Thompson River valley, Interior Plateau, British Columbia (2013-2020)

Abstract

The mandates of Inter-Departmental Letter of Agreement 4755 (IDLA-4755) and Inter-Departmental Memorandum of Understanding (IMOU-5170) between Natural Resources Canada (NRCan), Geological Survey of Canada (GSC), and the Transport Canada Innovation Centre (TC-IC) are to research and monitor landslides where vital railway infrastructure and operations, public safety, natural resources, and the environment are at risk. Research activities in the Thompson River valley railway corridor from 2013-2020 are reported herein, including: i) an ongoing proactive infrastructure monitoring and evaluation (PRIME) survey in collaboration with the British Geological Survey (BGS); ii) monitoring with a developmental global navigational satellite system (GNSS); iii) high-resolution photogrammetric change detection using unmanned aerial vehicles (UAV) and commercially available software; and iv) fine and ultra-fine resolution mapping of Thompson River using RADARSAT-2 and SENTINEL-1 synthetic aperture radar (SAR).

Keywords

Geological Hazards, Climate Change, Landslide Monitoring, Railway Infrastructure, Risk Reduction, Thompson River, British Columbia

Cover illustration: WorldView image with landslides of the Thompson River valley, British Columbia (north to bottom left of image); red dots indicate where railway infrastructure and operations are at risk from active landslides identified in this report

1. Introduction

Rail is the dominant transportation mode for moving Canada's export bulk natural resources (e.g., coal, grain, potash, forest products) to the Port of Vancouver, the third largest port in North America by tonnage and Canada's busiest container port. In 2017 alone, this port handled 142 million tonnes of cargo, including 3.25 million twenty-foot equivalents, which enabled the trade of approximately $200 billion in goods (portvancouver.com 2018 [URL]). Resilient railway transportation networks require sustainable, cost-effective management of service operations to meet future socioeconomic needs, and ensure protection of the natural environment. Where transportation corridors traverse unstable terrain, critical rail infrastructure is at risk of damage, and presents potential local and national economic, social and environmental challenges. Monitoring unstable slopes and infrastructure at risk is a cost-effective hazard management practice that also provides important geoscience information to help develop appropriate mitigation measures.

1.1 Landslides of the Thompson River valley, British Columbia

Vital railway infrastructure and operations are at risk from landslides across much of Canada. Particularly vulnerable sections of the Canadian National (CN) and Canadian Pacific (CPR) railway networks run through the Thompson River valley between Ashcroft and Spences Bridge in southern British Columbia (BC) (**Figure 1-1**). Sections of train track and other infrastructure traverse active landslides where gradual, continuous slope movements (and occasional rapid failures) affect the safety, reliability and resilience of railway operations. The economic importance of this transportation corridor, along with the need to understand and manage the safety risk related to the landslides that threaten this route, make the Thompson River valley a research priority for Natural Resources Canada (NRCan), Geological Survey of Canada (GSC), and the Transport Canada Innovation Centre (TC-IC), as mandated by Inter-Departmental Letter

of Agreement 4755 (IDLA-4755) and Inter-Departmental Memomorandum of Understanding (IMOU-5170).

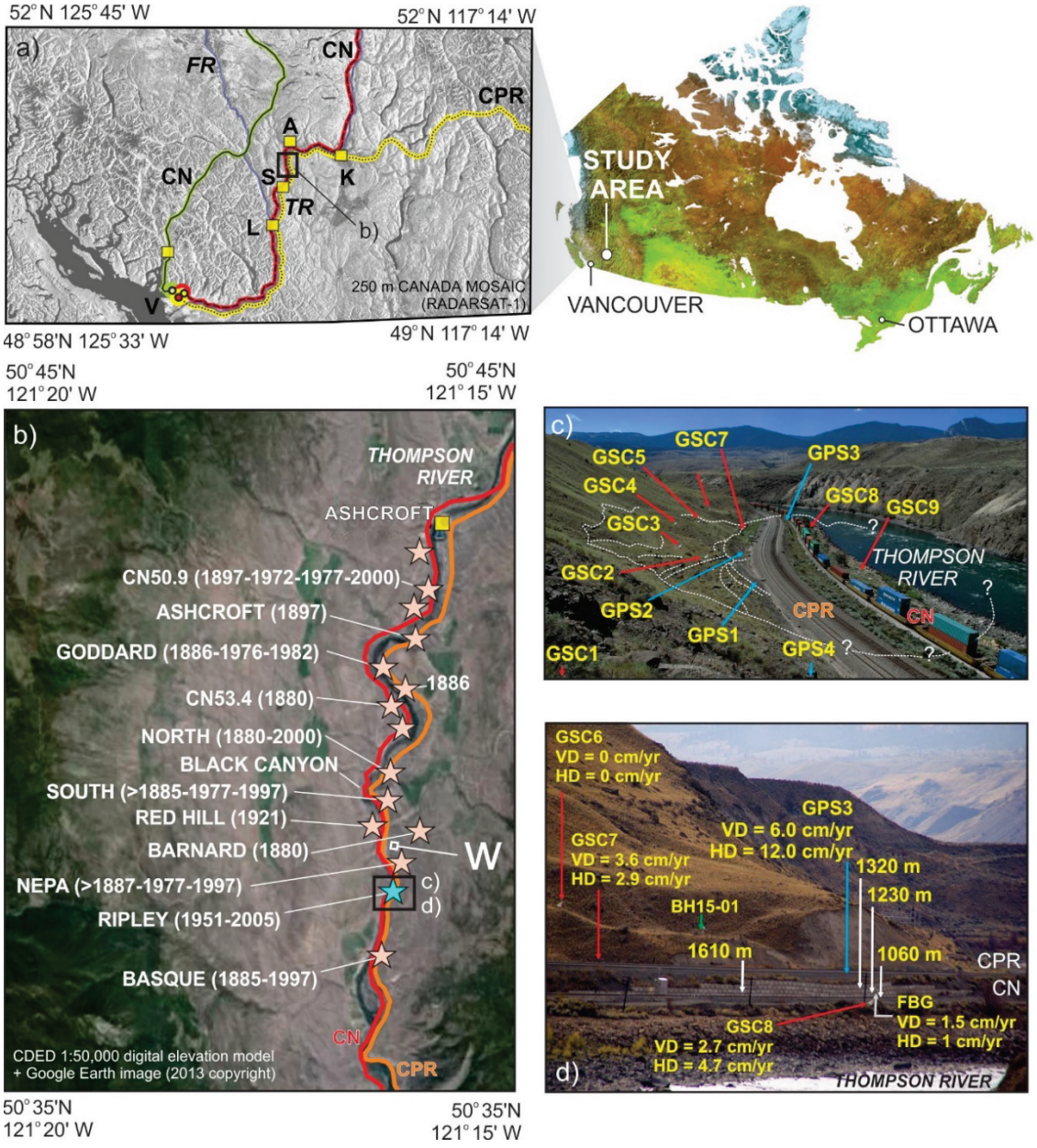

Figure 1-1 The study area. a) Rail transportation corridors (solid green, red and yellow lines) in southwestern British Columbia with location of the Thompson River valley area of interest: **A** – Ashcroft; **K** – Kamloops; **L** – Lytton; **S** – Spences Bridge; **V** – Vancouver; **FR** – Fraser River; **TR** - Thompson River (solid blue lines). b) Landslides of the Thompson River valley, with location of Ashcroft, the railway transportation corridor and Ripley Landslide test site; w – weather station location. c) Overview of the Ripley Landslide test site highlighting the location of GNSS monitoring stations (GPS1-4), InSAR corner reflectors (GSC1-9), and the monitored retaining wall dividing the CN and CPR tracks - view to south (NRCan photo 2020-290); d) South flank of landslide with sagging retaining wall separating CN and CPR tracks with displacement vectors for FBG, GNSS and InSAR stations; strain points detected by BOTDR (white arrows and distance in metres from datum); **VD** – vertical displacement; **HD** – horizontal displacement detected by FBG (grey arrow with displacement values expressed as mm/yr); and location of BH15-01 (green arrow) (NRCan photo 2020-291).

The GSC, together with international and national stakeholder-partners, has pioneered innovative monitoring of landslides in the Thompson River valley since 2013 **(Appendix 1**). These landslides serve as field-based laboratories to test and compare the reliability and effectiveness of different static, dynamic, and real-time monitoring technologies. Collaboration with other government agencies, universities, industry stakeholders, and international partners has been key to the successful delivery of the research activities (**Appendix 2**). Collaborative successes over the duration of the IDLA-4755 included: 1) real-time electrical resistivity monitoring with the British Geological Survey (BGS), Queen's University Belfast (QUB), and University College Dublin (UCD); 2) change detection with interferometric synthetic aperture radar (InSAR) in collaboration with the Canada Centre for Mapping and Earth Observation (CCMEO), University of Alberta (UA), University of Florence (UNIFI), Canadian industry partners (TRE-Altamira) and 3vGeomatics (3vG); 3) fibre optic strain monitoring in collaboration with the China Geological Survey (CGS); 4) real-time change detection with Geocubes™ in partnership with Ophelia-Kylia in France; and 5) the automation of the total weather station in collaboration with the University of Saskatchewan (USASK).

2. Current Research Activities (2013-2020)

Key R&D activities discussed in this section focus on geological, geophysical, and remote-sensing investigations that provide a wide range of key datasets on active landslides adversely impacting rail lines in the Thompson River valley transportation corridor. The rationale and key findings for each research activity are briefly summarized below, including details on methodology, results, and interpretations. Complementary datasets on landslide properties (e.g., geophysics, geomorphology, surficial geology, failure zone depth and geometry), slope activity (e.g., geomorphic change, GNSS-measured displacements, InSAR-measured displacements), and dynamic hydrologic conditions (e.g. soil moisture, precipitation, river level) allow researchers to: 1) determine landslide structures, composition, and failure mechanisms; 2) quantify spatial and temporal patterns of landslide activity (including changes in surface features, progressive creep, and possible development of more moderate or rapid failures); and 3) characterize environmental conditions that may influence landslide activity (such as river stage, precipitation and air/ground temperature). Comparison of these three forms of information provides insight on factors controlling slope activity in the region, and thus how to predict future slope failures. This knowledge will ultimately improve risk assessment by guiding activities such as risk avoidance, development of early-warning systems, and physical mitigation or adaptation.

2.2 ACTIVITY 1: Understanding the hydrogeophysical properties of Ripley Landslide (Collaborators: GSC, BGS, UA, USASK)

2.2.1 Landslide mapping and monitoring (2013-2020) and knowledge gaps

The primary research goal for this activity was to monitor differences in the geophysical properties of unconsolidated sediments and bedrock, interpreted in the context of the known lithological units on site (**Figure 2-1**; **Table 2-1**; Huntley and Bobrowsky 2014; Huntley et al. 2017a, b; Huntley et al. 2020a). Ripley Landslide occurs in unconsolidated valley fill on the east bank of Thompson River, and due to the small size (~3.3 ha) and continuous activity, it is an ideal target for geohazard characterization and monitoring (Fig. 1 c; Bobrowsky et al. 2014, 2017). To investigate the form and function of the landslide, we undertook a field-focused program combining hydrogeological mapping, stratigraphic analysis of borehole logs, geophysical testing (Huntley and Bobrowsky 2014; Huntley et al. 2017a, b), along with laboratory

characterization of sediments and their electrical properties (Holmes et al. 2018, 2019, 2020; Sattler et al. 2018). Newly characterized hydrogeological, geophysical variability, and electrical properties of the landslide provide important context for interpreting instrumental and remotely sensed records, and for understanding causal mechanisms and behaviour of this, and similar landslides in the Thompson River valley. This activity will also guide future monitoring and geohazard mitigation efforts in the BC interior, and other semi-arid settings where landslides are adversely affecting critical infrastructure in transportation corridors (Bobrowsky et al. 2018).

Collaborative research in this activity (**Appendix tables 1-1, 1-2 and 1-3**) is helping to explain how hydrogeological conditions influence the spatial and temporal patterns of surface water and groundwater flow; and how future changes in climate and landscape conditions might influence landslide activity along Thompson River, and unstable slopes in other semi-arid regions with similar biogeoclimatic conditions. Hydrogeological units (**Table 2-1**) are defined on the basis of lithofacies and landform associations, texture, sorting, colour, sedimentary structures, degrees of consolidation, stratigraphic contact relationships, geological age, and other distinguishing characteristics described at over 80 field stations and 11 boreholes on, and adjacent to, the landslide (Huntley and Bobrowsky 2014; Huntley et al. 2017a, b; Huntley et al. 2020a). Drainage classes and permeabilities are based on field assessments of porosity, unit thicknesses, earth material textures, penetrative planar structures, and slopes driving hydraulic gradients. Accounts of the surface and vertical (stratigraphic) distribution of hydrogeological units and landforms at Ripley Landslide and adjacent terrain, and more detailed unit descriptions are found in Clague and Evans (2003), Johnsen and Brennand (2004), Huntley and Bobrowsky (2014), Hendry et al. 2015, and Huntley et al (2020a). Key hydrogeological characteristics of these units are highlighted in **Table 2-1**.

Conventional and experimental continuous monitoring technologies at Ripley Landslide (**Figure 2-2**) record increased slope instabilty from late fall to early spring when river and groundwater levels are lowest (Macciotta et al. 2014; Hendry et al. 2015; Schafer et al. 2015; Journault et al. 2018). Four permanent global navigation satellite system (GNSS) monuments installed by CPR across the landslide in 2008 (**Figure 2-2**) recorded cumulative annual displacement around 100 mm/yr to 200 mm/yr, which peaked from late autumn to early spring (Bunce and Chadwick 2012; Macciotta et al. 2014; Hendry et al. 2015). Fibre Bragg grating (FBG) and Brillouin optical time domain reflectometry (BOTDR) monitoring of the retaining wall from 2013 to 2015 detected ~ 2 mm of accumulated strain in the wall, including displacement of individual blocks at its southern end, with peak activity occurring in the fall and winter months (Bobrowsky and Sladen 2013; Huntley et al. 2014; Huntley et al. 2016; Huntley et al. 2017b). Subsurface borehole monitoring combining ShapeAccelArray (SAA) inclinometry with piezometer head levels indicated that the main slide body is failing in highly plastic clay beds. These strata contain periodically groundwater-saturated sub-horizontal shear surfaces at depths between 5 m and 15 m below surface. The central and northern parts of the slide translate sub-horizontally (2.1° to 2.5°,), whereas the southern portion near the lock-block retaining wall has a steeper (28°) slide surface (Macciotta et al. 2014; Hendry et al. 2015; Schafer et al. 2015).

On their own, surficial mapping and landslide change detection monitoring reveal limited information on the subsurface range of earth materials, structures, and hydrological behaviour. Although earth material stratigraphy, textures, and penetrative planar structures are important controls on sub-surface porosity, permeability and hydrology, and hence landslide activity in the Thompson River valley, it remained unclear how these factors influence the style, timing, and rate of slope displacement (i.e., form and function). For

this research activity, geophysical methods, deployment of soil moisture and weather sensors, and laboratory techniques are combined and tested to address these knowledge gaps.

Table 2-1 Hydrogeological units of Ripley Landslide (see also **Figure 2-1**)

Stratigraphic unit	Geological notes
Unit 10	Ballast, culverts, and lock-block retaining wall separating CPR and CN tracks – see **Figure 2-1 k,l**
Unit 9	Alluvial floodplain sediments (post-glacial): boulders, cobbles and sand, sparse vegetation growth dominated by horsetails indicating zone of seepage across the landslide toe – see **Figure 2-1 j**
Unit 8	Colluvial sediments (post-glacial): erratic boulders, glaciofluvial cobbles and sand remobilized by debris fall, soil creep and surface runoff on slopes ranging from 25º slope above the headscarp to 12º across the main slide body; on steeper portions of the slope (up to 32º), talus blocks are derived from frost shattered rhyolite and volcaniclastic rock – see **Figure 2-1 i**
Unit 7	Alluvial fan sediments (post-glacial): silt, sand and gravel deposited on outwash and till as terraced fans with slopes up to 12º; indicate falling base levels in the Thompson River valley during early Holocene – see **Figure 2-1 h**
Unit 6	Glaciofluvial sediments (glacial retreat-phase): cobble gravel and sand; moderately steep slope (25 º - 32º) is gullied and drains a 340 m - 350 m elevation terrace abutting against bedrock (unit 1b) – see **Figure 2-1 g**
Unit 5	Glaciolacustrine sediments (glacial retreat phase): interbedded silt and clay overlying till (unit 4), silt-rich beds appear lighter; bedding-parallel fissility and vertical slope relaxation fractures formed in exposed in railway embankment – see **Figure 2-1 f**
Unit 4	Subglacial till (glacial maximum): massive, matrix-supported diamicton overlain by a veneer of hillslope colluvium (unit 8) exposed in headscarp at 280 m elevation – see **Figure 2-1 e**
Unit 3	Glaciolacustrine sediments (glacial advance-phase): rhythmically interbedded clay, silt and sand with rare dropstones; sub-till (unit 4) soft-sediment indicates glacial deformation (ca. 278 m elevation) – see **Figure 2-1 d**
Unit 2	Colluvial sediments (glacial retreat-phase): interbedded clast-supported diamicton, sand and gravel overlying fractured bedrock (unit 1) (ca. 276 m elevation) – see **Figure 2-1 c**
Unit 1b	Flow-banded rhyolite and pyroclastic volcanic rock; strike/dip/dip-direction 104º/18º/E (350 m elevation) – see **Figure 2-1 b**
Unit 1a	Fine-grained crystalline andesite with dominant fractures 040º/076º/E, 074º/50º/NNW, 136º/78º/W, 178º/28º/E (278 m elevation) – see **Figure 2-1 a**


unit 1a
a)
d)
unit 3
unit 2
c)
b)
unit 1b
f)
unit 5
e)
(oldest) 340 m ---
300 m ---
285 m ---
(youngest) 280 m ---
unit 6
g)
unit 7
h)
unit 4
unit 8
unit 9
unit 10
k)
j)
i)
unit 10
l)

Figure 2-1 Hydrologeological units of Ripley Landslide – see also **Table 2-1** (Huntley and Bobrowsky 2014; Huntley et al. 2020a) a) Unit 1a- andesite: fine-grained crystalline igneous rock with dominant fractures 040º/076º/E (278 m elevation), 074º/50º/NNW, 136º/78º/W, 178º/28º/E (NRCan photo 2020-292). b) Unit 1b - rhyolite and pyroclastic volcanic rock: strike/dip/dip-direction 104º/18º/E (350 m elevation) (NRCan photo 2020-293). c) Unit 2 – colluvial sediments: interbedded clast-supported diamicton, sand and gravel overlying fractured bedrock (unit 1), ca. 276 m elevation (NRCan photo 2020-294). d) Unit 3 - glaciolacustrine sediments: rhythmically interbedded clay, silt and sand with rare dropstones; sub-till (unit 4) soft-sediment indicates glacial deformation, ca. 278 m elevation (NRCan photo 2020-295). e) Unit 4 – lodgement till: massive, matrix-supported diamicton overlain by a veneer of hillslope colluvium (unit 8) exposed in headscarp; at 280 m elevation (NRCan photo 2020-296). f) Unit 5 - glaciolacustrine sediments: interbedded silt and clay overlying till (unit 4), silt-rich beds appear lighter; bedding-parallel fissility and vertical slope relaxation fractures formed in exposed in railway embankment (NRCan photo 2020-297). g) Unit 6 - glaciofluvial sediments: cobble gravel and sand; moderately steep slope (25 º - 32º) is gullied and drains a 340 m - 350 m elevation terrace abutting against bedrock (unit 1b) (NRCan photo 2020-298). h) Unit 7 - alluvial fan sediments: silt, sand and gravel deposited on outwash and till as terraced fans with slopes up to 12º; indicate falling base-levels in the Thompson River valley during early Holocene (NRCan photo 2020-299). i) Unit 8 - colluvial sediments: erratic boulders, glaciofluvial cobbles and sand remobilized by debris fall, soil creep and surface runoff on slopes ranging from 25º slope above the headscarp to 12º across the main slide body; on steeper portions of the slope (up to 32º), talus blocks are derived from frost shattered rhyolite and volcaniclastic rock (NRCan photo 2020-300). j) Unit 9 - alluvial floodplain sediments: boulders, cobbles and sand, sparse vegetation growth dominated by horsetails indicating zone of seepage across the landslide toe (NRCan photo 2020-301). k) Unit 10 - anthropogenic features: boulder-rich track ballast overlying alluvial floodplain on the landslide toe; CN (top left) and CPR tracks (centre) (NRCan photo 2020-302); l) Unit 10 - lock-block retaining wall separating CPR (above left) and CN tracks (right) (NRCan photo 2020-303).

2.2.2 Geophysical methods and monitoring (2013-2020)

Geophysical surveys were undertaken between 2013 and 2015 using a combination of terrestrial and waterborne electrical resistivity tomography (ERT), frequency domain electromagnetic conductivity measurements (FEM), ground-penetrating radar (GPR), seismic pressure wave refraction (PWR), and multichannel analysis of surface waves (MASW) (Parry et al. 2014; Bauman et al. 2015; Theriault et al. 2017). Down-hole measurement of natural gamma radiation (GR), induction conductivity (IC) and magnetic susceptibility (MS) were also collected in boreholes located directly adjacent to the CPR tracks (**Figure 2-2**; Gugins and Candy 2015). Geophysical traverses were spaced across the breadth of the landslide and Thompson River to ensure reasonable diversity in coverage of subsurface variability (**Figure 2-2**). Terrestrial cross-sections constructed in November 2013 extended from above the landslide head scarp to the channel bank. River survey lines (November 2014) trended parallel to the shoreline, and were traversed using a metal-hulled jet boat towing a non-metallic white-water raft containing the geophysical equipment (Bauman et al. 2015).

With regard to geoelectrical properties, five terrestrial ERT lines used a Wenner-Schlumberger array with 48 electrodes spaced 5 m apart. Four waterborne ERT lines used a reverse Wenner array with an electrode spacing of 10 m that was dragged behind the jet boat, floating on the river surface (Huntley et al. 2017a; Huntley et al. 2019a; Holmes et al. 2019; Holmes et al. 2020). Apparent resistivity datasets were merged into a single file and interverted using the RES3DINV inversion program (Huntley et al. 2019b). A proactive infrastructure monitoring and evaluation (PRIME) resistivity monitoring system was installed on the Ripley Landslide in November 2017 (Holmes et al. 2018). This system, which provides near-real time 4-D resistivity data, consisted of two intersecting Wenner arrays (one 91 m long with 45 electrodes, the other 54 m long with 27 electrodes, all evenly spaced). The PRIME system was connected to the internet via a modem and allows for remote data acquisition. Environmental and instrumental limitations of the geophysical surveys were addressed in Huntley et al. (2017a) and Huntley et al. (2019a, b).

The importance of soil matric suction (i.e., negative pore water pressure) on slope instability has long been recognized (Holmes et al. 2018; Sattler et al. 2018): soil suctions increase the strength of soil and help stabilize slopes. However, transient near-surface changes in matric suction pressures because of climatic conditions may be sufficient to induce slope movement. In November 2017, two Decagon MPS6 soil suction meters were installed in the headscarp of Ripley Landslide to a depth of 2 m; another three experimental meters were installed in November 2018 (**Figure 2-2**). The use of resistivity as a proxy for suction is evaluated in this study (Sattler et al. 2018; Holmes et al. 2020).

2.2.3 Results and discussion

An unprecedented level of insight into the internal composition and structure of the landslide has been gained from the terrestrial, waterborne, and borehole geophysical surveys (**Figure 2-3**). Of all the geophysical techniques, ERT surveys provide the most complete and deepest penetrating information regarding the internal structure of the landslide (Huntley et al. 2017a, b; Huntley et al. 2019a, b), and are the focus of the discussion. The terrestrial-based ERT survey undertaken in November 2013, and waterbourne ERT survey completed in November 2014, are presented with PRIME data from November 2018 in a fence diagram showing the range of electrical properties of the landslide (**Figure 2-3**). Since the surveys were completed at the same time of year, differences arising due to the influence of seasonal changes in weather conditions on the electrical properties were minimised. Selecting November as the month of observation ensures that the electrical properties are comparable, although completed in different years. Data from the terrestrial-based ERT lines were inverted in 3D using Res3DInv (Holmes et al. 2018), taking account of the offline variation in topography in the topographically complex area of the slide. This improved the correlation between each of the lines, reducing the mismatch in resistivity values at depth. The waterbourne survey data were inverted in 2D using Res2DInv (Huntley et al. 2020a).

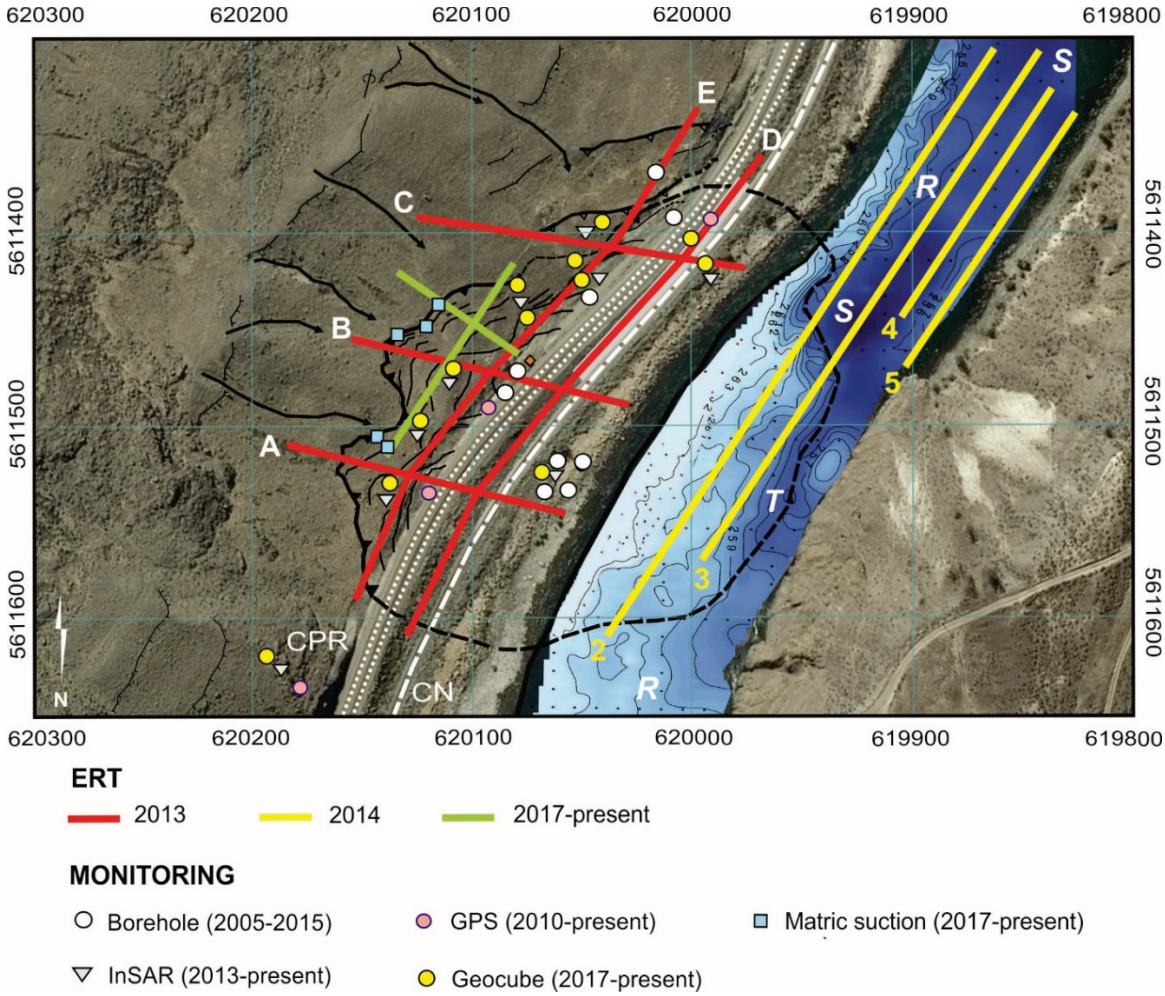

Figure 2-2 Geophysical transects for November 2013 (red lines), November 2014 (yellow lines), and PRIME installation, beginning in November 2017 (green lines); other monitoring components shown include positions of logged boreholes (2005-2015), InSAR corner reflectors (2013 - present) and permanent GNSS stations (2010 – present). CPR signals bungalow – orange triangle. Ripley Landslide boundary - solid black lines with downslope teeth; tension cracks – thin solid black lines; projected extension - dashed black lines; gullies (with drainage direction) - solid black arrows; post-glacial terraces - solid lines with downslope ticks. Thompson River bathymetry grades from dark blue (250 m elevation) to white (263 m elevation) at the landslide toe (Huntley et al. 2017a). Channel morphology: *R* – riffle (bedrock high); *T* – thalweg scour (glacial sediemnts in bedrock basin at landslide toe); *S* – scour pool (glacial sediments in bedrock basin at landslide toe). Projections of geophysical results require that UTM grid north is oriented to the bottom of the figure; grid squares are 100 m x 100 m.

Combined terrestrial and waterborne 2D ERT datasets are visualized as a pseudo-3D model of resistivity values using ParaView® software (**Figure 2-4**). Pseudo-3D models capture resistivity, soil moisture and groundwater conditions in surficial deposits and bedrock for the fall seasons of 2013 and 2014 (**Figure 2-3** and **Figure 2-4**). This representation is interpretation-oriented, with the selection of resistivity thresholds at 80 Ωm and 110 Ωm determined by observations of earth materials, and their hydrogeological properties at surface, and in logged boreholes. Competent bedrock (unit 1, **Figure 2-1 a**) has a high resistivity value, >110 Ωm (**Figure 2-4**). Weathered bedrock and colluviated fine-grained beds at the base of unit 2 (**Figure 2-1 b**) are moderately resistive (80 Ωm to 110 Ωm). Overlying areas with low resistivity values (<80 Ωm) are correlated with the oldest Pleistocene glaciolacustrine sediments, units 2 and 3 (**Figure 2-1 c, d**). Unit

4, subglacial till, appears as a moderately resistive (80 Ωm to 110 Ωm) silt, clay and boulder diamicton up to 5 m thick (**Figure 2-1 e**). Silt-rich glaciolacustrine sediments (unit 5, **Figure 2-1 f**) have low resistivity values (<80 Ωm). Overlying glaciofluvial outwash (units 6 and 7, **Figure 2-1 g, h**) are moderately resistive (80 Ωm to 110 Ωm) when undersaturated (dry). Coarse, rapidly drained colluvium (unit 8) has a high resistivity value >110 Ωm (**Figure 2-1 i**). Modern alluvial floodplain sediments (unit 9, **Figure 2-1 j**) are saturated (wet) through much of the year and return high resistivity values (Fig. 6). Coarse ballast (unit 10), when undersaturated (dry), has a high resistivity >110 Ωm (**Figure 2-1 k, l**).

Downhole natural GR levels, IC, and MS surveys of boreholes BH15-01, BH15-02, and BH15-03 (**Figure 2-3**) provide further insight into the sub-surface thickness of earth materials, depth to bedrock, groundwater conditions and failure mechanisms of the landslide. East of the CP tracks, the Mount Sopris MGX logging tool encountered 15 m to 17 m of glacial deposits overlying basal bedrock in the boreholes (**Figure 2-4**). West of the CN tracks, boreholes show approximately 30 m of till and clay-rich glaciolacustrine sediments overlying bedrock (**Figure 2-4**). These observations corroborate the terrestrial and waterborne geophysics results indicating the main landslide body is located over a >20 m deep bedrock basin underlying the modern Thompson River. Natural GR logs show a relatively constant response (**Figure 2-3**), interpreted to indicate the predominance of clays in the glacial deposits. Minor changes in readings throughout the borehole reflect small variations in sand, clay and silt content, and levels of uranium, thorium, and potassium in granitic and arkosic dropstones (units 2 and 3) and erratics (in unit 4) directly adjacent to boreholes. The IC logs show an initial progressive, but subtle rise in conductivity values (**Figure 2-3**) corresponding to an increase in clay content with depth. High conductivity zones may indicate clay horizons in silt- and boulder-rich till (unit 4). At depth, conductivity levels fall in response to a lower clay content at depth (unit 3), decreasing porosity in stiff to hard silt-clay diamicton (unit 2), and electrically resistive bedrock intersected in the bottom of boreholes (unit 1). The MS logs show a consistently low response (**Figure 2-3**) indicating a very low ferromagnetic mineral content in the surrounding glacial deposits (units 2 to 5). The slight decrease in MS apparent near the base of each borehole corresponds to the intersection of unconsolidated glacial deposits with fractured, weathered andesite bedrock (**Table 2-1**).

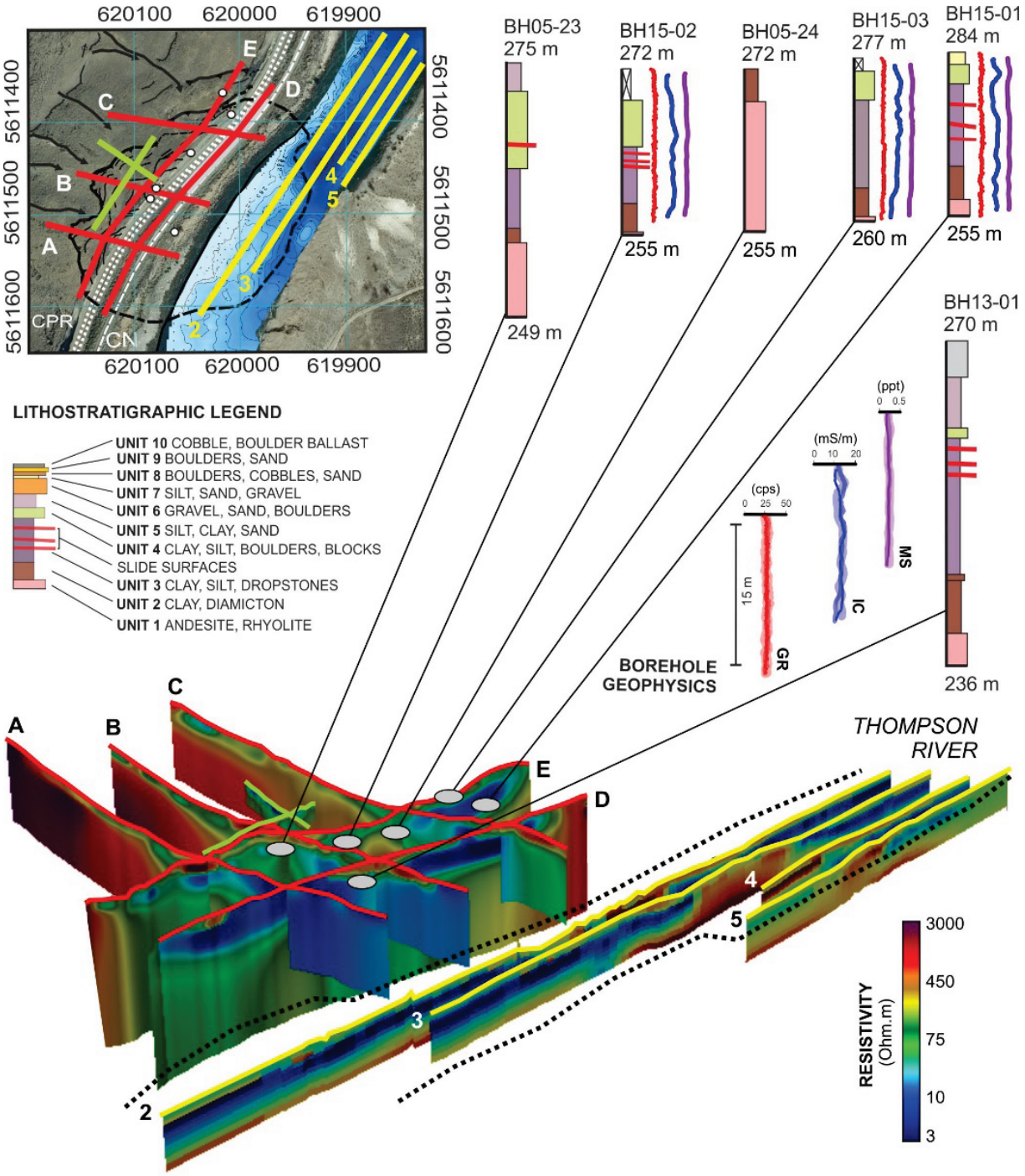

Figure 2-3 Terrestrial ERT pseudosections (red transect lines A, B, C), waterborne ERT pseudosections (yellow transect lines 2, 3, 4, 5) and PRIME installation (green transect lines). Location of boreholes shown in relation to transect lines. Gamma radiation measured in counts per second (cps), induced conductivity measured in milliSiemens/m (mS/m) and magnetic susceptibility in parts per thousand (ppt)**.** Also shown, location of elevated terrain conductivity readings located on submerged slide toe. Landslide extent (approximate) shown as dashed black lines on inset map.

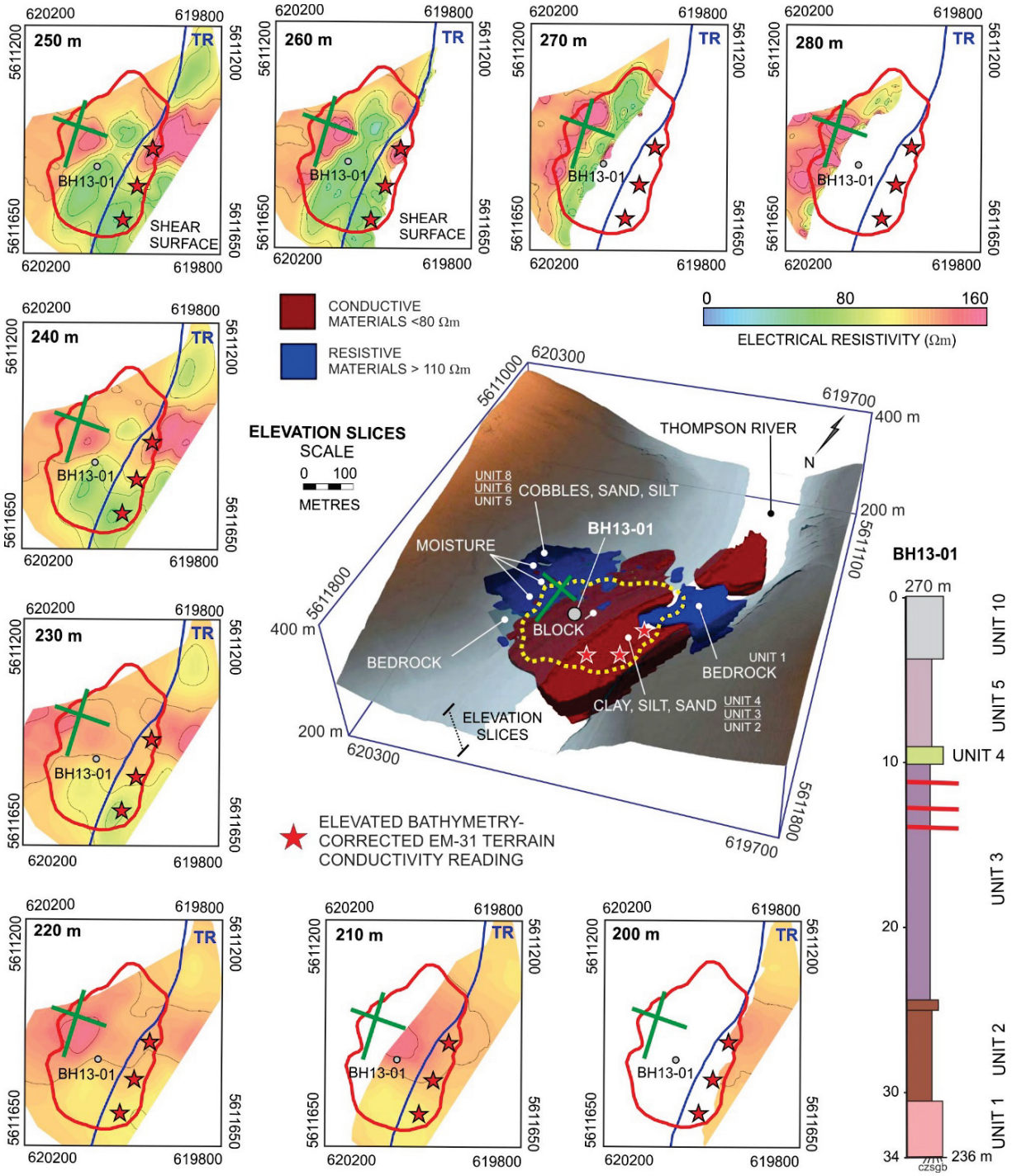

Figure 2-4 Electrical resistivity tomographic depth slices of Ripley Landslide. Location of BH13-01 shown; graphic log captures changes in hydrogeological units at depth near the centre of the slide body. Solid blue line – east bank of Thompson River (**TR**). Solid green line - PRIME array. Red stars indicate elevated bathymetry-corrected EM terrain conductivity interpreted as artesian groundwater discharge zones exposed by river erosion. Data processing by Frontier Geosciences Inc.

The PRIME system provides new insight into the hydrogeological structure and function of the slope, imaging surface tension cracks >0.5 m-wide, and 1 m-deep penetrating units 8 and 4, and extending to landslide failure planes in units 2 and 3 (**Figure 2-5**). Field suction-resistivity relationships were established by relating the resistivity of the head scarp as revealed by the PRIME data with sensor data from the head scarp. The daily average soil suction is plotted alongside the daily average resistivity of the cells in the resistivity model corresponding with the suction sensor depth. The location of the suction sensor is shown in **Figure 2-2 and Figure 2-5**. Although readings of the soil suction sensors for a range of depths up to 2 m below the surface are averaged, results are dominated by the sensor at 0.3 m depth with the largest magnitude of suctions. Results reflect the non-linear relationship of soil suction with moisture content, and dependence of resistivity on moisture. Generally in winter, resistivity and suction increase as moisture content decreases (**Figure 2-6**). A deviation from this trend is observed mid-January when daily resistivity was higher than expected. This is likely due to localized freezing at the surface resulting in increased resistivity, which is supported by the weather station data showing temperatures below 0°C around this time (**Figure 2-6**). Therefore, there is an increase in resistivity despite effective rainfall being positive during this period, which is usually associated with decreased resistivity. Large decreases in surface resistivity (>50%) from March to May are due to an increase in moisture content accompanying snowmelt and intense, short-duration precipitation events. Temperatures are consistently above 0°C by this time, and despite a negative weekly effective rainfall during this season (**Figure 2-6**), the additional moisture resulting from snowmelt is sufficient to increase the moisture content of the slope. The propagation of the wetting front along the failure plane is clearly shown in **Figure 2-5**, indicating that the headscarp acts as a major conduit for the flow of percolating groundwater over this interval.

Peak displacement rates in the Thompson River valley are observed through winter to spring, indicating that low river and groundwater levels do not account for all movement. Ground-control cameras (**Figure 2-6**), and the climate monitoring station (**Figure 2-7**) record that between late fall (November) and early spring (March), snowfall blankets the slope, while the ground freezes to an estimated depth <2 m as air temperature stays consistently below 0°C. When air temperatures are >0°C, rain and melting snow result in an increase in moisture content of sub-surface clay-rich units (Huntley et al. 2019b, c). The greatest displacement rates indicated by GNSS and InSAR (see Section 2.3) occur during winter and spring when transitional ground conditions allow snow melt and rainfall to penetrate deep into the still-frozen (or thawing) slide body by way of tension cracks, planar fractures and bedding surfaces. During summer months, Thompson River levels are high and support the submerged portions of the toe slope. Groundwater is at its maximum level within the slide body. Short intervals of intense, heavy rainfall rapidly infiltrates through the surface soils, or is lost to evapotranspiration and overland runoff. It is during this period that GNSS and InSAR monitoring indicate minimum rates of surface displacement (Huntley et al. 2018a; Huntley et al. 2019c; Huntley et al. 2020b**)**.

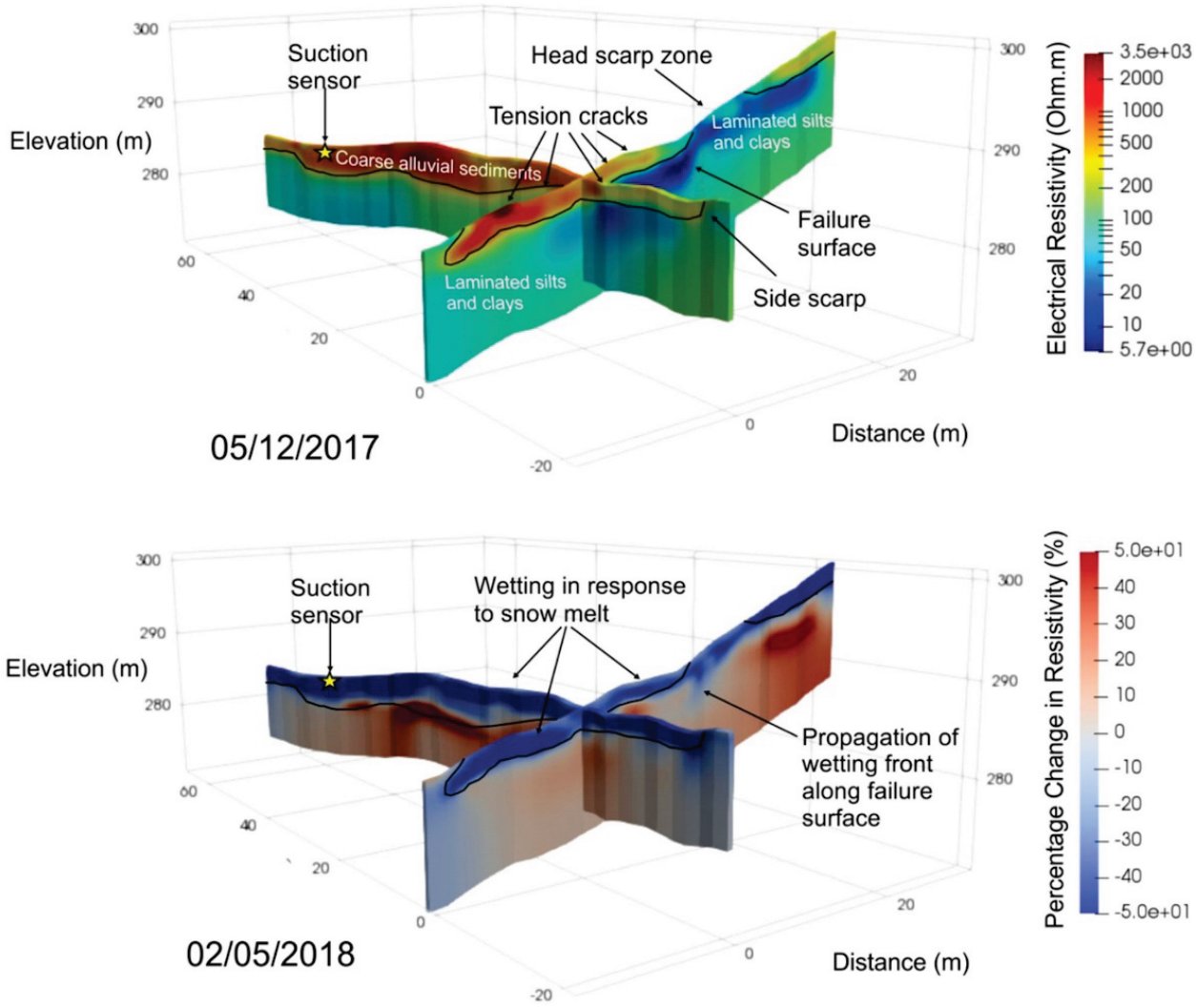

Figure 2-5 Electrical resistivity tomographic images generated from the PRIME data collected on the Ripley landslide. The baseline image (December 05, 2017) highlights the lithological units present on site and shows key geomorphological features including failure surfaces and tension cracks. The image from May 02, 2018 shows the percentage change in resistivity from the baseline image, highlighting changes that took place following the onset of snowmelt on the site. Yellow stars mark suction sensor locations. The suction sensors (yellow star) are located at 0.3 m, 0.6 m, 0.9 m, 1.2 m and 2 m below the surface.

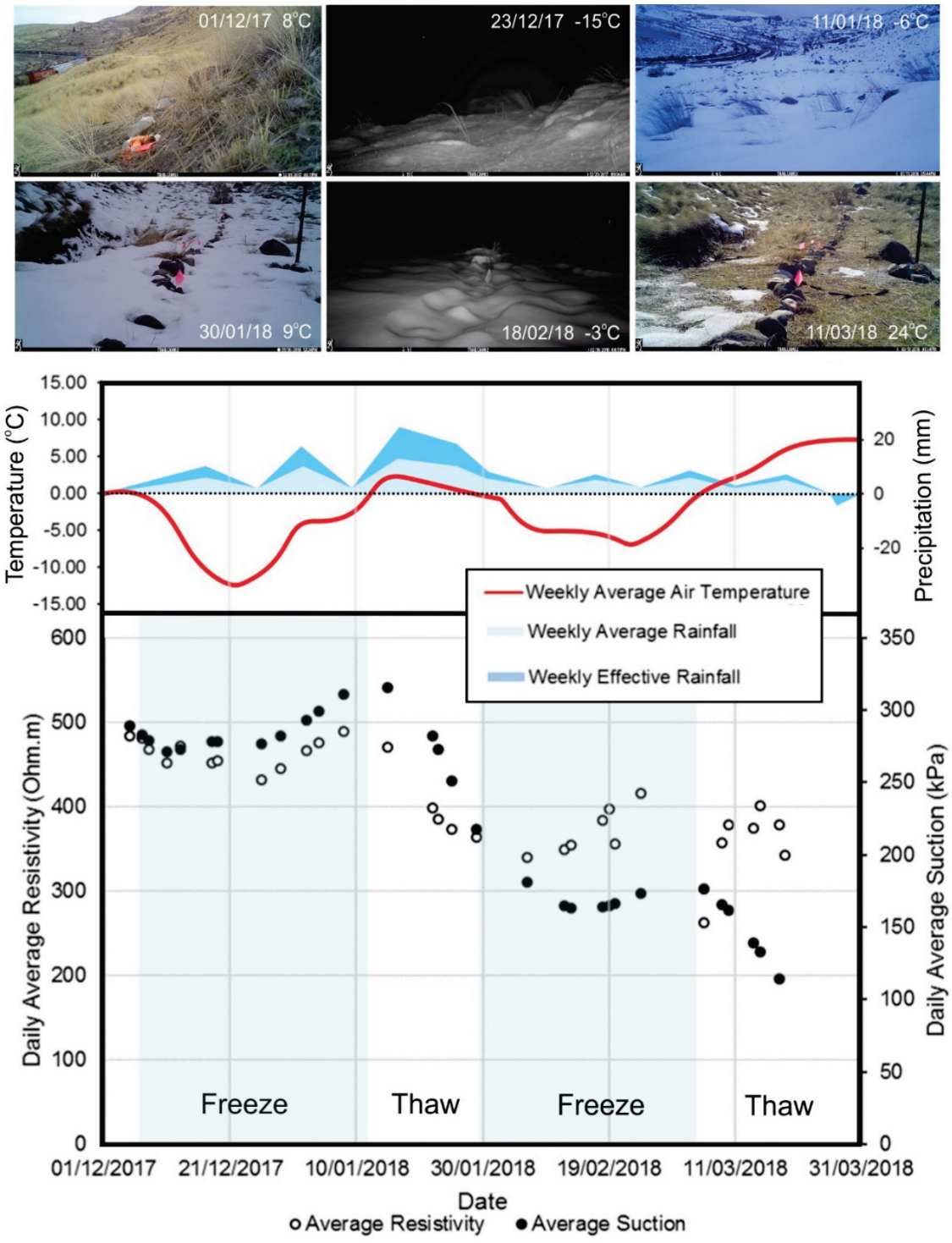

Figure 2-6 Ripley Landslide ground conditions from December 2017 to March 2018, with the relationship between resistivity and suction for the head scarp. The average daily resistivity is the average resistivity of cells of the PRIME model (**Figure 2-5**) proximal to the suction sensors (within 1 m distance). Suction sensors located at 0.3 m, 0.6 m, 0.9 m, 1.2 m, and 2 m below the surface; **Figure 2-5** shows the location relative to the PRIME ERT lines. Weather data recorded at the GSC climate monitoring station (**Figure 2-7**).

2.3 ACTIVITY 2: Evaluation of spaceborne, airborne, and ground-based change detection and monitoring technologies in the Thompson River valley (Collaborators: GSC, UA, USASK)

2.3.1 Geospatial monitoring (2013-2020), knowledge gaps, and solutions to test

A critical knowledge gap for landslide forecasting and risk reduction is our lack of understanding of the spatial and temporal distribution of movement/displacement from year to year in the Thompson River valley. Near real-time warning systems require detailed analysis of landslide motion combining sub-centimetre accuracy positioning in three dimensions with monthly, diurnal, or hourly temporal resolutions. However, periodic and continuous monitoring of ground control points (GCPs) and railway infrastructure with small and slow annual displacements (<10 cm/year) is particularly challenging in an environment with a semi-arid intermontane climate, and an extreme temperature range of -30°C to +40°C. For this collaborative activity (**Appendix 1** and **2**), the research goal is to evaluate the agreement and reliability of ground motion measurements from several complimentary landscape monitoring technologies under harsh environmental conditions in the south-central Interior Plateau (**Figure 2-2; Figure 2-7 a, b**). Multi-year datasets from real-time kinematic (RTK) GNSS surveys, continuous monitoring multi-frequency GNSS stations, and a network of single frequency GNSS sensors (Geocubes™) are compared with displacement measurements obtained from Structure from Motion (SfM) analysis using imagery acquired from Unmanned Aerial Vehicles (UAV), and persistent scatterer (PS) interferometric synthetic aperture radar (InSAR) results.

2.3.2 Methods of investigation and monitoring limitations

This section outlines the methods of change detection monitoring deployed at the test site to improve the spatial and temporal resolution of slope deformation. In common with other InSAR studies of unstable slopes, for the Thompson River valley, interferometric analysis of RADARSAT-2 imagery provides spatially expansive records of motion of landslides, but has low accuracy, and is restricted to line-of-sight components and observation intervals limited by orbital paths (Huntley et al. 2014; Huntley et al. 2017c, Journault et al. 2018; Huntley, et al. 2020b). GNSS systems capture three-dimensional displacement vectors with high temporal resolution, and so complement remote sensing techniques, providing baseline surface mapping datasets and measures of landslide activity (Macciotta et al. 2017; Rodriguez et al. 2018; Huntley et al. 2020b).

2.3.2.1 Real-time kinetic GNSS surveying (terrestrial and bathymetric)

Rigorous change detection requires an accurate and precise elevation model to serve as a reference base map. In 2008, CPR installed four permanent GNSS monuments trackside across the landslide (**Figure 2-2**; **Figure 2-7 a**). These monuments record cumulative annual displacements >10 cm/yr to <60 cm/yr, with peak movement in winter (Macciotta et al. 2014; Hendry et al. 2015); and captured the 2017 displacement event, recording 47 cm/yr at the north end of the slide, and 52 cm/yr on the lock-block retaining wall. Two areas of maximum displacement recorded by the GNSS stations coincide with maximum displacement indicated by the InSAR corner reflectors (**Table 2-5**). The larger zone spans the CN and CPR tracks between GSC3 to GSC5, GPS1 and GPS2, and GSC9. A smaller zone is centred on GSC7, GPS3, and GSC8 at the south end of the landslide near the lock-block retaining wall (**Figure 2-7 a**).

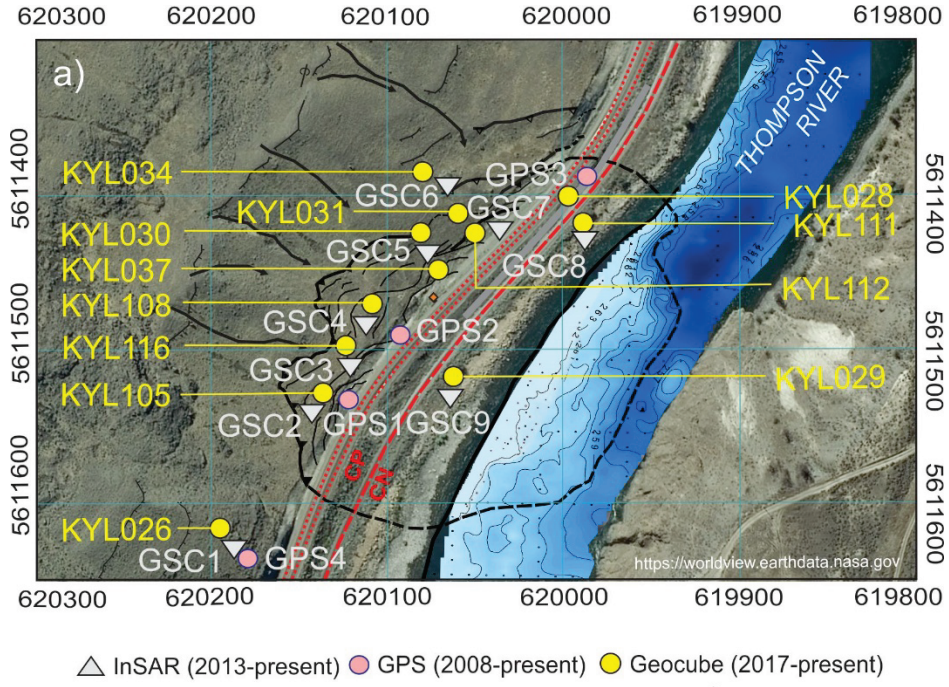

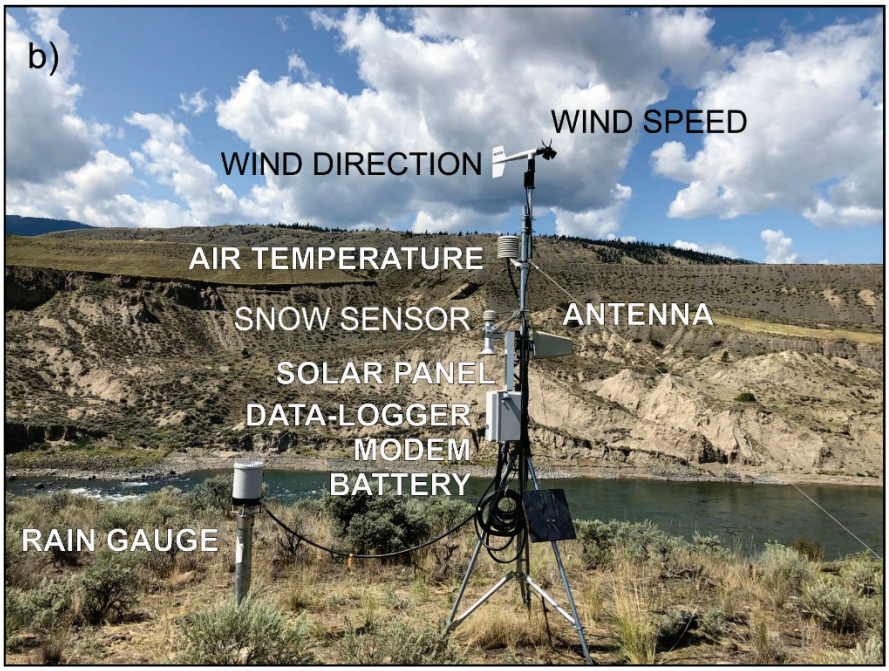

Figure 2-7 a) Plan view of the test site highlighting the location of GNSS monitoring stations (GPS1-4), InSAR corner reflectors (GSC1-9) and Geocubes™ (KYL026 to KYL116). Railway infrastructure: Canadian National track - red dashed line; Canadian Pacific tracks – red dotted lines; monitored lock-block retaining wall dividing the CN and CPR tracks - light grey solid line. Bathymetry derived from GPR and single-beam acoustic depth soundings (modified from Huntley et al. 2017a). b) Weather station installed in 2016, and continuously recording climate variables since; see Figure 1c for location (NRCan photo 2020-304).

In 2016, permanent ground control points (GCP) were established across the slope, using stable boulders and anthropogenic features on, and adjacent to the landslide (**Figure 2-8 a**). Subsequently, positional data were referenced using the North American datum (NAD83) and Universal Transverse Mercator (UTM) Zone 10. From 2016 to 2017, surveys used RTK-GNSS receivers: Ashtech NovAtel DL-V3, EOS Arrow Gold, and Trimble R10 GNSS units. After 2018, surveyed points were positioned using two Spectra Precision SP-80 receivers (**Figure 2-8 b**). Under optimal conditions, at least ten Global Positioning Systems (GPS), and Globalnaya Navigazionnaya Sputnikovaya Sistema (GLONASS) satellites were visible, and typically between 14 and 17 satellites were accessible. A reference base station was established on a stable post-glacial terrace near Black Canyon, 3 km north the Ripley Landslide (**Figure 2-1 c**). The absolute position of the station was determined from a post-processed RINEX file using the Canadian Spatial Reference System (CSRS) Precise Point Positioning (PPP) tool after a nine-hour occupation. Reported absolute positional accuracy was 0.8 cm horizontally and 1.3 cm vertically (95% sigmas), and used for all surveys (**Figure 2-8 a**). All GNSS positioning data were reviewed, corrected for antenna laybacks, heights and edited for erroneous data points during the data processing (Huntley et al. 2017a; Huntley et al. 2020c, in review).

Between 2014 and 2018, GPR, single-beam acoustic, and multi-beam sonar bathymetric surveys were completed at Ripley Landslide; and a 10 km reach of Thompson River from Ashcroft to Basque Landslide (Bauman et al. 2015; Young et al. 2017; Huntley et al. 2018b; Huntley et al. 2020, in review). High-precision bathymetric data was collected through the study reach with a BioSonics® DTX hydro-acoustic Echo Sounder equipped with an integrated sensor to correct depth data for variable transducer orientations experienced in turbulent flow (November 2014, March 2017), and a Norbit wide multi-beam integrated sonar (October 2017, November 2018). Transducers were mounted midship, or off the starboard side of the swim board at the stern of a 5 m-long aluminum-hulled jet boat. Depth data were collected by traversing the study reach at approximately 100 m intervals and along the shoreline while moving between transects. Data collection were limited in shallow water or high velocity rapids. To provide high-precision data, the net speed of the boat was maintained between 5 km/h and 8 km/h against the strongly flowing river. Each survey day, water level at the Ashcroft boat launch was measured using a rover EPOCH 50 RTK receiver. The RTK rover was used to measure water surface, wetted width, and bank elevations up to the high-water mark at channel gradient changes (e.g., upstream and downstream ends of rapids where data quality was poor or absent), and where bathymetric surveying coverage was acceptable. The additional bank and water surface elevation data were used to assist with tying bathymetric data into UAV digital surface models. Bathymetric data were recorded on a Panasonic Toughbook using Visual Acquisition software (Version 6.1). EchoVIEW software (Version 7.1) was used to post-process and correct raw data to create bathymetric maps throughout the study reach. Positional control for waterborne surveys was provided using a Trimble GeoExplorer 6000 series hand-held GNSS unit, the GPS/GLONASS receiver in a Garmin EchoMAP 50s, and the Garmin Sounder 188 GNSS. Positioning data were confirmed using a Garmin 60cs hand-held GNSS and EPOCH 50 RTK GNSS receivers. Bathymetric surveying ended early for to ensure the safety of crew and equipment after the Norbit system hit a large submerged boulder, shearing mounting column and injuring a field crew member.

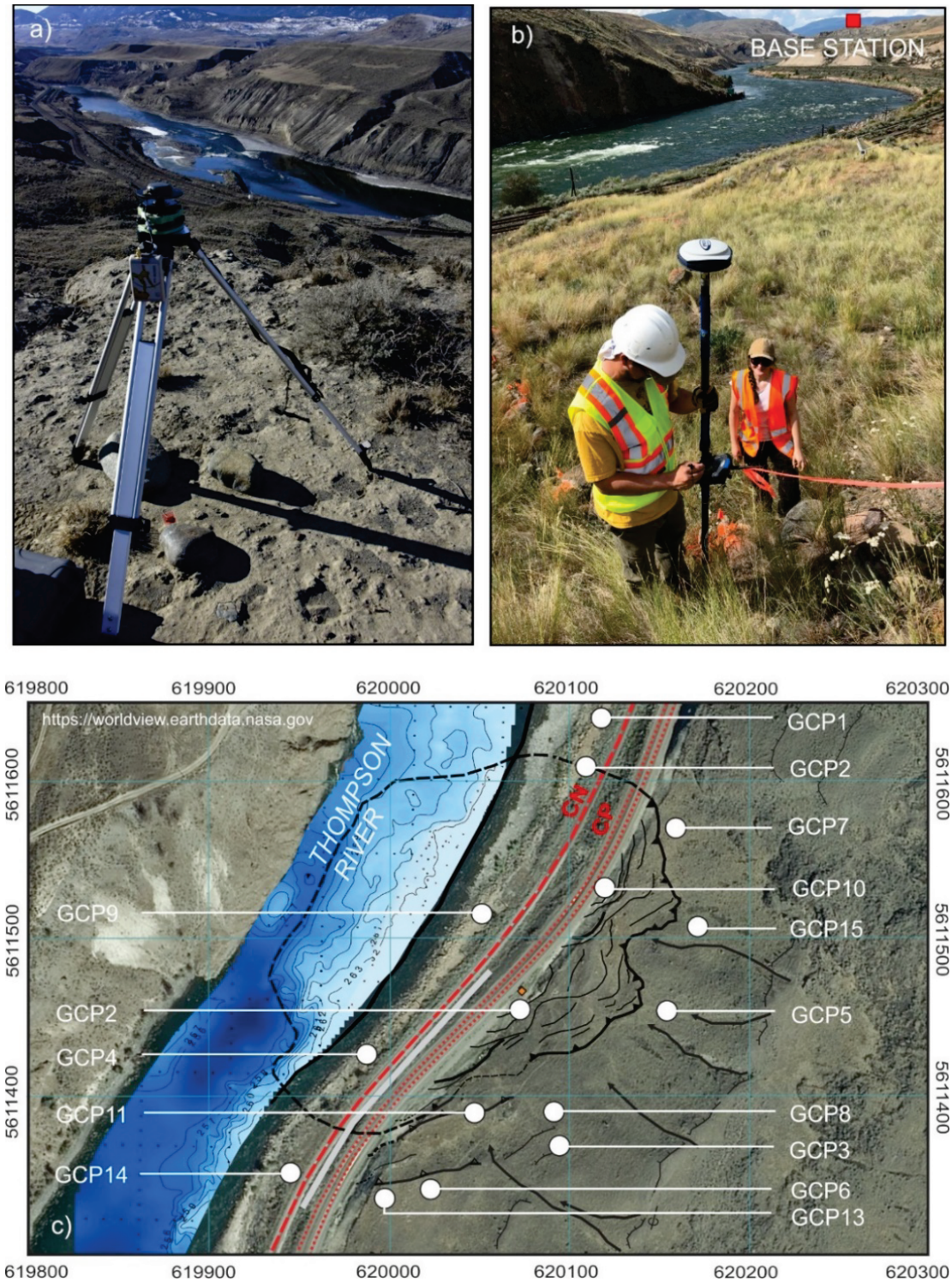

Figure 2-8 a) Base station at South Slide, with EOS Arrow Gold base unit positioned over the prime GCP (March 2019) (NRCan photo 2020-305); b) Trimble Spectra SP-80 RTK GNSS head and Spectra TSC3 Ranger handheld computer (NRCan photo 2020-306); c) distribution of ground control points (GCPs) on and adjacent to Ripley Landslide. Note, grid north is to the top of the map.

2.3.2.2 Differential GNSS monitoring with Geocubes™

Repeat RTK-GNSS surveys generates point position data across much of the slide body. However, this method provides limited information on the seasonal variation in displacement rates and amounts. Different GNSS (d-GNSS) monuments installed by CPR provide continuous, near-real-time monitoring of surface displacement, but only at three trackside locations (**Figure 2-7 a**). Starting in 2016, a high-resolution (millimetric) Geocube (GeoKylia)™ GNSS network was installed at Ripley Landslide to address both issues of spatial and temporal coverage (Macciotta et al. 2017; Rodriguez et al. 2018; Holmes et al. 2020, in press; Huntley et al. 2020, in review). This monitoring system comprised twelve small, rugged, single-frequency d-GNSS transmitter-receivers with directional antennas (Geocube™) that relayed geospatial data to a Geocoordinator unit hosting a proprietary operating system developed and provided by Ophelia Sensors in France. A 3G network modem with an omnidirectional antenna provided internet access to the Geocoordinator (**Figure 2-9 a**).

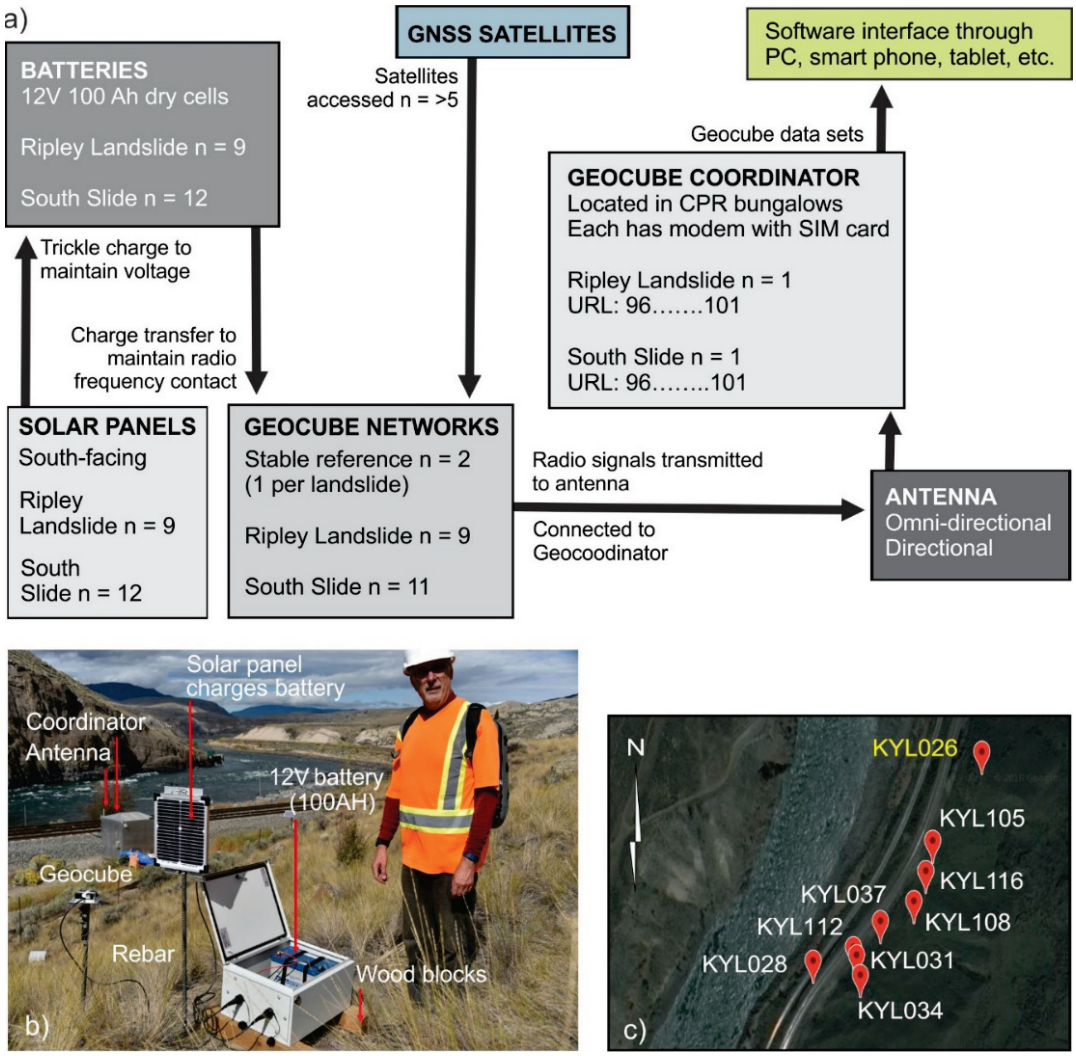

Figure 2-9 Geocubes™ installation: a) schematic of Geocube™ system; b) components installed on the unstable slope (NRCan photo 2020-307); c) Geocube™ network installed at Ripley Landslide (yellow text label is stable reference position).

For installation, at each monitoring location (**Figure 2-9 b**), a 1 m length of steel rebar was first driven into the soil to a maximum depth of 75 cm. A Geocube™ was mounted on an aluminum plate and attached to the rebar by means of pipe clamps and adhesive tape. An alternative mounting approach was to attach the plate and Geocube™ to a nearby InSAR corner reflector. The second method ensured Geocubes™ had a wide horizon to receive satellite signals. Units were levelled by using spacing washers and a locking nut; then oriented in the line-of-sight with the antenna side pointing toward the Geocoordinator. Care was taken to ensure that each d-GNSS antenna had their line-of-sight cleared of vegetation. A second, 1.5 m length of rebar was driven to a maximum depth of 75 cm to allow the mounting of a 50 cm^2 solar panel. The mount was angled to allow solar panels maximum exposure to the sun when oriented facing south (**Figure 2-9 b**). For Ripley Landslide, one Geocube™ was installed on stable terrain adjacent to stations GSC1 and GPS4: a bedrock outcrop that confined the landslide in the northeast (**Figure 2-7 a**); the remaining eleven were positioned across the slide body to capture spatial variation in displacement (**Figure 2-9 c**). Radio signals were reflected by anthropogenic obstacles between the coordinator, reference site, and Geocubes™ (e.g., rolling stock, tracks, and lock-block retaining wall).

Because of the remote location, a requirement for the Geocube™ system was low power consumption. The monitored slopes face WNW, and were overshadowed by the surrounding hillsides making solar panels unsuitable sole power sources for system components. Ruggedized, rechargeable 12V 100Ah Lead-acid batteries were selected as a more reliable power source to drive the monitoring systems, with recharging facilitated by the solar panels. Batteries were housed in either a weatherproof steel, or high-impact plastic box with four-pin and two-pin electrical sockets for the attachment of a Geocube™ unit and solar panel (**Figure 2-9 b**). Battery voltages between 11 Volts and 15 Volts were required for optimal performance. A disadvantage of employing ground-based instrumentation was that units often experienced damage attributed to local wildlife (e.g., bears, deer, cattle, rats, snakes). Within two months of initial installation at Ripley Landslide, cables were damaged on a number of units. Wildlife cameras established the chief culprits to be a herd of deer grazing on the rangeland. After some experimentation, the most cost-effective and animal-proof approach was to cover exposed cable with a combination of tightly-woven fine wire mesh, 2 mm-thick spiral-wound plastic tubing, and rubberized adhesive electrical tape.

2.3.2.3 Unmanned Aerial Vehicle surveying

UAVs allow flexible, inexpensive acquisition of low-altitude aerial imagery, whereas various off-the-shelf photogrammetric software packages enable production of high-resolution digital surface models (DSM) from such images. Beginning in September 2016, repeat UAV surveys of Ripley Landslide, using the GSC-owned DJI Phantom 4, have aimed to capture changes in landslide morphology (**Figure 2-10**). Plan-view and oblique colour aerial photographs were merged using SfM software, and DSMs then generated at a resolution of 2 cm (**Figure 2-10 c, d**). UAV survey flight planning was conducted using Pix4D Capture (2016, 2017) and Map Pilot (2018, 2019); the SfM modelling was undertaken using Pix4D Mapper.

Planimetric displacement of the landslide was first mapped using an ENVI 5.2 plug-in called Cosi-Corr (co-registration of optically sensed images and correlation) developed by the California Institute of Technology. The co-relation was conducted on hill-shaded UAV DSMs of the landslide created on September 2016 to September 2017, and September 2017 to October 2018. Hill-shading was applied at 1.5 times exaggeration and 310° azimuth and 45° sun altitude. Areas of vegetation, and recent track ballast work

on hill-shaded images were masked using ArcMap 10.5 prior to correlation to reduce the areas with substantial change not related to slide movement. Two images were created for E/W (X) and N/S (Y) displacement. Elevation changes (Z) were calculated in ArcMap using map algebra applied to the SfM-derived DSM. Maps of 3D displacement maps were calculated by squaring each image (X, Y, Z) to convert all measurements to positive. These values were then added and squared to produce a single raster containing 3D displacement values that were all positive (larger values = more displacement). Horizontal displacement *vectors* were derived using Cosi-Corr and applied using the E/W and N/S images. The final images were coloured in ArcMap 10.5 (Huntley et al. 2020c, in review).

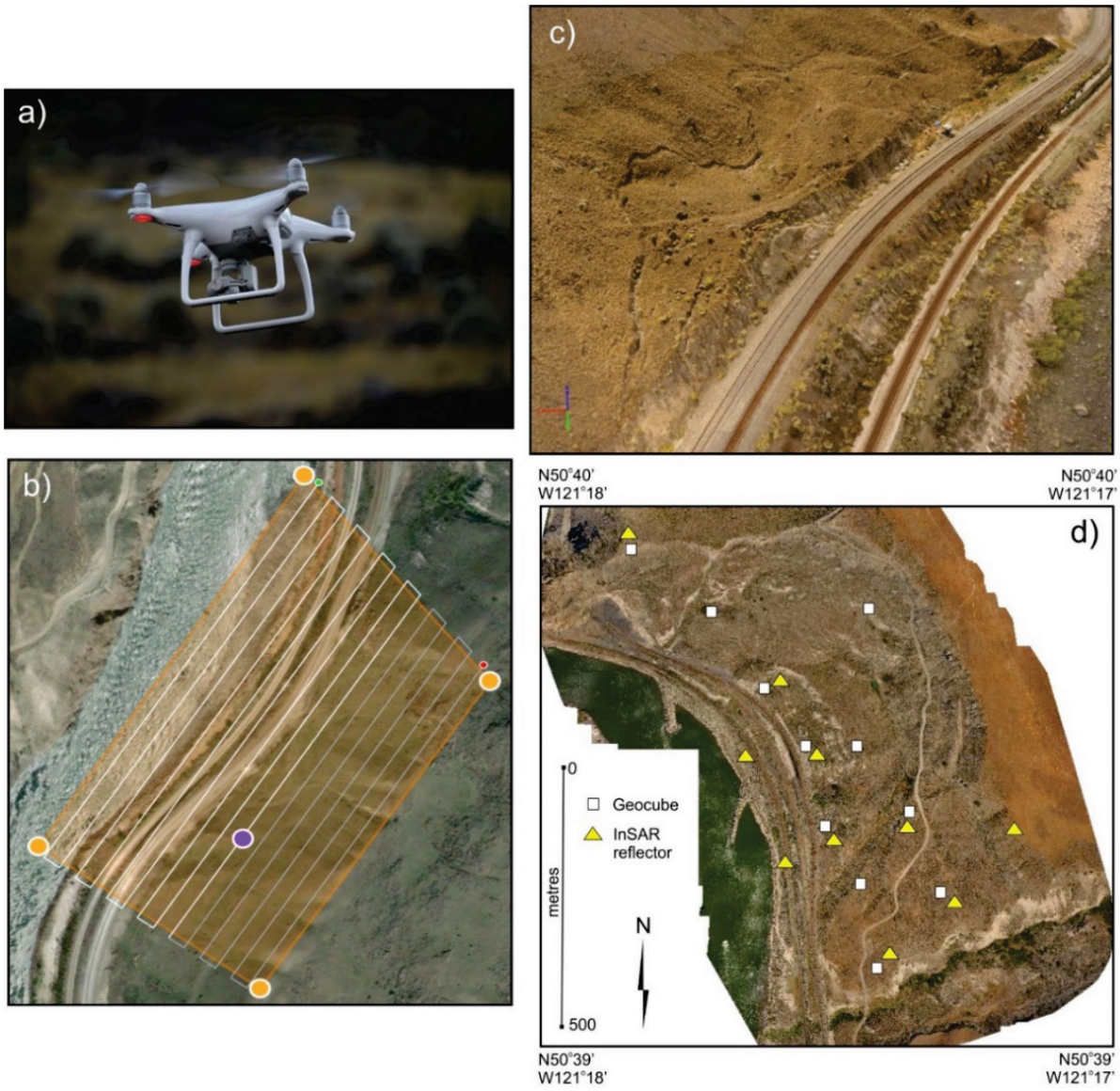

Figure 2-10 a) DJI Phantom 4 UAV (GSC photo 2020-308); b) Programmed flight plan for Ripley Landslide September 2019 survey, north to top of scene (image: P. Skrivanos); c) DSM of Ripley Landslide generated by SfM software (September 2016), view to south; d) DSM of South Slide generated by SfM software, showing location of InSAR corner reflectors and Geocubes™ (September 2017).

2.3.2.4 InSAR acquisition and analyses

Ground motion measured by spaceborne InSAR produce results with precision comparable to d-GNSS measurements, but have the advantage of monitoring displacement over large areas (e.g., Huntley et al. 2017c; Journault et al. 2018). Remote sensing is effective in the Thompson River valley as a first approximation for determining ground hazard susceptibility, and whether site investigation is warrented. Additional testing is required before RADARSAT-2 can be broadly used for change detection across Canada. Datasets must be compared along with other satellite platforms, low-cost remote change detection monitoring techniques employing unmanned aerial vehicles (UAVs), geophysical investigations (e.g., electrical resistivity tomography, ERT), and bathymetric surveys.

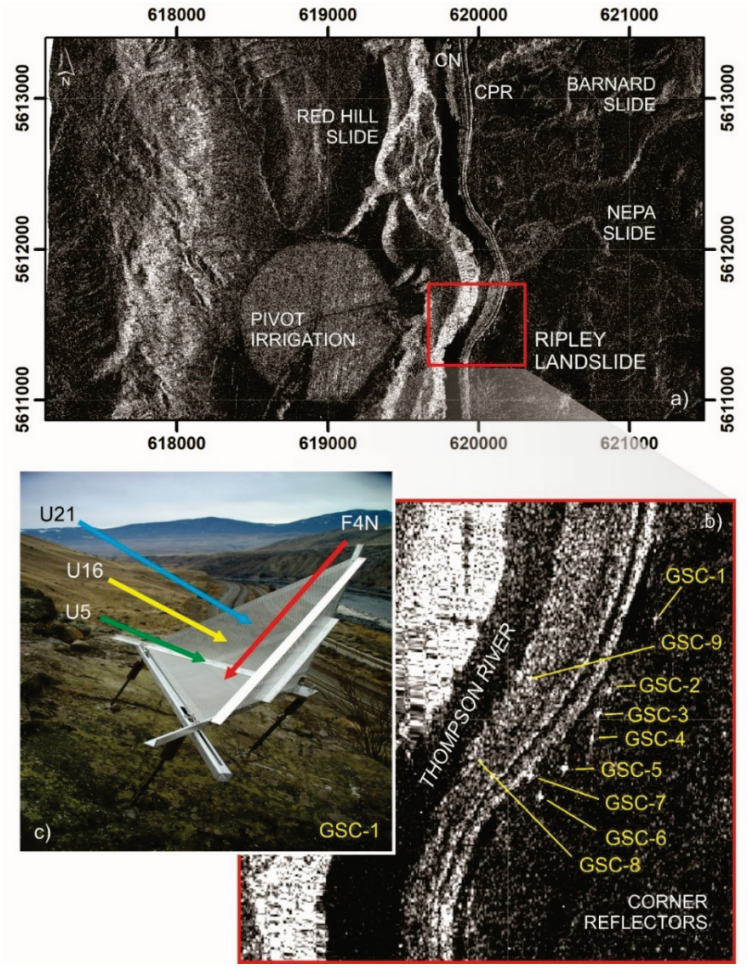

Figure 2-11 a) Regional orthorectified RADARSAT-2 SAR amplitude image, showing Ripley Landslide in relation to other slow-moving landslides and major anthropogenic features in the Thompson River valley; b) orthorectified amplitude image of Ripley Landslide, showing trihedral corner reflectors (GSC-1, master stable reflector on bedrock); c) stable trihedral corner reflector (GSC-1) showing diagrammatic Ultrafine beam paths for three descending nodes along an azimuthal line-of-sight of 280° (U5 34°, U16 42°, and U21 45°), interferograms were generated from a stack of U21 images; corner reflectors are not oriented to utilize the ascending node along an azimuthal line-of-sight of 088° (F4N 44°) (NRCan photo 2020-309).

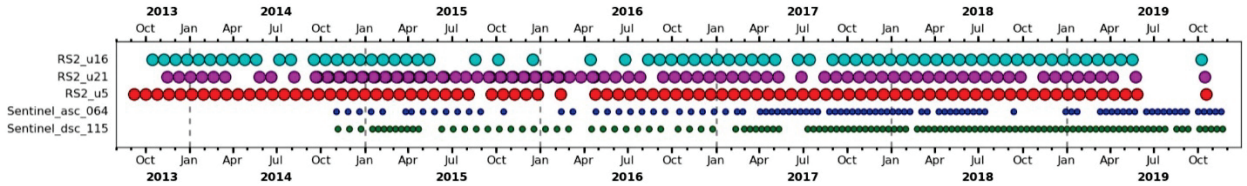

Figure 2-12 Raster coverages of SENTINEL-1 and RADARSAT-2 scenes used in comparison by 3vGeomatics (Pon et al. 2020).

PCI Geomatica (2018) was used to create a series of interferograms from a stack of U21 Ultrafine RADARSAT-2 images (**Figure 2-11 a**). The stack has an average incident angle of 45.4°, and was acquired with a right-looking geometry from descending orbital passes east of the study site. Reliable InSAR targets were identified from the stack of SAR imagery by examining the degree of phase stability over time for every resolution cell within the study area (**Figure 2-12**). By considering only targets with persistent scatterer characteristics, and correcting for phase change contributions caused by orbital position errors, topography and atmospheric effects, a time series of deformation for each target was recovered with possible measurement accuracies of several mm (cf. Henschel et al. 2015). The trihedral corner reflectors (**Fig. 2-11 b, c**) installed on site served as highly coherent artificial InSAR targets. Submillimeter accuracy of corner reflector time series' has been demonstrated experimentally (Ferretti et al. 2007). For stack pre-processing, SAR imagery was co-registered with a geo-coded DEM derived from airborne LiDAR. Temporary coherent targets were identified across scenes. Multi-master interferograms were created (minus winter scenes) with atmospheric effects removed. Signal enhancement included proprietary partner pixel searching and adaptive filtering. Network processing included: unwrapping, displacement rates, and height error estimation by 3vGeomatics (Pon et al. 2020).

2.3.3 Results and discussion

2.3.3.1 Static real-time kinetic GNSS surveying (terrestrial and bathymetric)

A total of 15 GCPs are positioned on stable boulders and anthropogenic features (**Figure 2-7 a**). Large changes in Z values (~15 m) between 2017, 2018 and 2019 surveys are related to a datum shift at the prime GCP, and so have been excluded from further discussion. Five GCPs record significant horizontal displacement on the landslide (**Table 2-2**). Upslope of the train tracks, on the main slide body, GCP10 records 8.7 cm of movement to the NNW; and GCP12 captures 16.1 cm of NW displacement. Downslope of the tracks across the slide toe, 11.3 cm of WNW displacement is measured at GCP02; GCP04 is displaced 16.4 cm NW; and GCP09 moved 18.3 cm NW over the two-year observation period (**Table 2-2**). The remaining GCPs are on stable portions of the slope, and adjacent to the landslide (**Figure 2-7 a**).

Below water level, high-resolution single-beam, multi-beam acoustic, and GPR bathymetric surveys provide details of surface morphology and sub-surface composition, respectively. Provisional results (**Figure 2-13**) show multi-beam bathymetry layered in ArcGIS, on a World View satellite image, and merged with other change detection datasets. Bathymetric data acquired for the active Ripley Landslide between 2014 and 2018 establishes the river bed geometry, and identifies river-bottom erosion at the slide toe (Huntley et al. 2018). Many boulder diffractions are visible in the GPR cross-section (Huntley et al. 2017d). No obvious stratigraphy, sedimentary structures or sediment packages can be interpreted on the GPR cross-section due to the boulder diffractions in the modern fluvial sediments. Results of the 2017 and 2018 multi-beam surveys reveal variations in river bed composition ranging between fines draping bedrock

to coarse gravel and boulders overlying clay-rich valley fill. The resolution of the Norbit system is sufficient to identify boulders, suggesting this system is adequate for repeat surveys to map changes in river-bottom profiles.

Table 2-2 Ground control points (GCPs) recording horizontal displacement in centimetres (Δ Northing, Δ Easting) from September 2017 to September 2019.

UTM Zone 10	Northing	Easting	Northing	Easting
SURVEY DATE	**GCP-02**		**GCP-04**	
30/9/2017	620101.7468	5611603.802	619983.3499	5611431.344
30/6/2018	620101.7912	5611603.862	619983.2662	5611431.423
30/10/2018	620101.754	5611603.889	619983.238	5611431.433
15/08/2019	620101.716	5611603.892	619983.206	5611431.473
30/09/2019	620101.729	5611603.913	619983.192	5611431.483
Δ N / Δ E	**1.7798 cm**	**-11.118 cm**	**15.7943 cm**	**-13.93 cm**
SURVEY DATE	**GCP-09**			
30/9/2017	620045.3471	5611522.005		
30/6/2018	620045.3272	5611522.063		
30/10/2018	620045.278	5611522.085		
15/08/2019	620045.221	5611522.132		
30/09/2019	620045.23	5611522.145		
Δ N / Δ E	**11.7065 cm**	**-14.018 cm**		
SURVEY DATE	**GCP-10**		**GCP-12**	
30/9/2017	-	-	620072.3907	5611451.301
30/6/2018	620116.6772	5611533.564	620072.3152	5611451.367
30/10/2018	620116.651	5611533.579	620072.308	5611451.359
15/08/2019	620116.609	5611533.598	620072.262	5611451.398
30/09/2019	620116.595	5611533.59	620072.3907	5611451.301
Δ N / Δ E	**8.2157 cm**	**-2.605 cm**	**12.8706 cm**	**-9.651 cm**

Single- and multi-beam bathymetric datasets capture key river-bed features, including the thalweg channel and scour pools at the toe of Ripley Landslide and South Slide, a >50 m deep scour pool in Black Canyon, and (significantly) other active and inactive slides (**Figure 2-13**). Scour features at landslide toes are also revealed in more detail with the multi-beam data. Clay-rich sediments appear to be exposed at base of scour pool, with a depth of 15 m. Shallow waters are revealed with rapids adjacent to stable terrain, separated by deep (typically 5-10 m below river level) scour pools adjacent to the toes of all landslides in the Thompson River valley.

The November 2014, March 2015, October 2017, and November 2018 river surveys reveal variations in bed composition ranging from sand and silt draping bedrock, to coarse gravel and boulders overlying clay-rich valley fill. Shallow waters (riffles) with rapids lie adjacent to stable terrain, separated by deep scour pools (typically 5-10 m below river level) adjacent to the toes of all landslides. This pool-riffle channel pattern reflects the intersection of the modern river channel with bedrock and deposits of glacial, boulder-rich clay preserved in deep paleochannels segments along the studied reach, and suggests that fluvial erosion plays a key role in the location of major slope instabilities. The channel bottom morphology was likely a significant pre-condition for slope failure in the late 19th Century (Stanton 1898; Clague and Evans 2003). Understanding the erosional regime at these stable slide toes will help us understand whether they could possibly reactivate in the near future. The discovery of scour pools incising landslide toe slopes are important for two reasons. Firstly, erosion within the pools removes support at the toes of the landslides,

likely contributing to their instability. InSAR interferometry, UAV photogrammetry, and d-GNSS markers confirm parts of the landslides close to the water edge have significant movement, and these active parts are typically in proximity to deep pools (**Figure 2-11**). Secondly, the scour pools can expose fractured and porous sediments at the river bed, improving hydraulic connectivity between the river and groundwater in the slide mass. Both of these apparent relationships will be investigated in more detail in the coming years as part of IDLA-4755 using multi-beam technologies. These remote bathymetric mapping techniques are thus important for expanding characterization of landslides toes where they are extrapolated to extend under Thompson River, and in developing a complete understanding of form and function.

Figure 2-13 Bathymetry and landslide history of the Thompson River valley (after Clague and Evans 2003), showing location of Ashcroft and railway transportation corridor in relation to the Ripley Landslide test site (yellow text and dot); prime ground control point, survey base station (red square); weather station (**W**). Bathymetric survey by Young and Slater (2017).

Similar to the other ground- and aerial-based surveys conducted at the site, mapping the river bottom has introduced another set of challenges as a result of the harsh operating environment. Extreme weather conditions, and very low river levels over the winters of 2016-2017 and 2018-2019 produced operational safety concerns, limiting surveys to the thalweg (i.e., the longitudinal path of greatest depth down the channel). With fast currents and white-water conditions, the jet boat is pitched, rolled, and yawed more than typical watercraft. Single-beam inertial measurement units (IMU) are too slow to accurately record the rapid changes in attitude, for example the scour features at landslide toes (e.g. Ripley Landslide). Some scour pools (e.g. Black Canyon, >45 m) are too deep for strong single-beam acoustic signal returns. The multibeam system provides complete coverage, but only for the slide areas in deeper water (pools). Surveying is not possible in rapids and in shallow waters (i.e. riffles) where the sonar system is confused by air bubbles caused by the current and turbulent water. This produces a considerable noise requiring post-survey manual clean-up of data. Shallow water requires a large number of passes, increasing the

likelihood of bottoming-out and damaging equipment. GSC are currently processing data collected for all bathymetric surveys (single- and multi-beam datasets).

2.3.3.2 Differential GNSS monitoring with Geocubes™

Differential GNSS data are used to help understand the behaviour and drivers of slope instabilities affecting rail transport in the Thompson River valley. Detailed examination of Geocube™ records provide insight on the rates and spatial pattern of creep, as well as the timing, and possibly precursors of changes in creep behaviour. To this end, the Geocube system is helping to characterize three-dimensional ground displacement patterns across Ripley Landslide (and at South Slide). This improved characterization of slope activity can then be combined with more spatially detailed line-on-sight displacements measured by InSAR and UAV photogrammetry. In addition, Geocube™ data is helping to evaluate the utility of precipitation, ambient temperature, and soil moisture in predicting landslide activity based on comparison of three-dimensional displacement measurements with PRIME results and meteorological records.

Geocubes™ displacement results from November 2018 to June 2019 are discussed here. Eight units installed across Ripley Landslide were active to some degree, and recording 3D displacement during this time interval (**Figure 2-6**; **Figure 2-14**). Three units were not active due to wildlife damage or low battery charge (KYL029, KYL030, KYL111). Geocube™ location data (X - longitude, Y - latitude, Z – height above sea level) collected over the eight month-long observation trial were imported into an ArcGIS Geodatabase. Geocube™ tracks are plotted as points, grey-shaded from light to dark according to date (per month) from exported individual Shapefiles (**Figure 2-14**).

Immediately apparent is the generally NW displacement trend for all working Geocubes, with each unit charting a helical drift over the months of observation (**Figure 2-14**). The exception is the fixed unit, KYL-00026, which shows no horizontal and vertical displacement over the eight month observation period. These trends are consistent with the displacement vectors derived from change detection analysis of InSAR, and UAV imagery. The “molecular” or “signature” tracks are a reflection of precision and accuracy of satellite data used and their orbital paths; daily and seasonal atmospheric conditions; which satellites are visible to antennas; and developing instrumental failure in some instances. Filtering and data smoothing removes some of this temporal drift. Using a 15 day moving average provides useable data from the Geocubes (cf. Rodriguez et al. 2018; **Figure 2-15**). As the network continues to collect data over the coming months and years, it is expected that the displacement paths will become better defined. KYL-00031 and KYL-00034 failed in late November; while KYL-00105 and KYL-00116 behave erratically; and KYL-00028 on the lock-block retaining wall functions intermittently.

Geocubes at the north end of the landslide capture movement at varying rates from November 2018 to June 2019, suggesting displacement of multiple slide blocks with shallow dipping slide planes. The most northerly moved horizontally NW 55.49 mm while dropping 18.75 mm in elevation (KYL-00105). A second block, forming a graben, moved NW 44.84 mm with a 16.60 mm drop in elevation (KYL-00116). The third block moved horizontally NW 50.26 mm, dropping 7.35 mm (KYL-00108) over the eight month trial. In the centre and south, generally slower horizontal, but greater vertical displacements were recorded over the eight month observation period. KYL-00031, positioned below the southern head scarp, moved horizontally NW 1.17 mm prior to failure during the winter. KYL-00037 captured 31.72 mm horizontal movement to the NW with a drop of 62.17 mm in a central block of the slide main body (the greatest vertical downward displacement across the slide body). Similar to KYL-00116 in the northern sector of the slide

body, KYL-00112 is located in a graben toward the southern margin of the slide. While experiencing only 34.40 mm of horizontal movement NW, the Geocube dropped 15.54 mm in elevation. On the lock-block retaining wall, KYL-00028 recorded 39.01 mm of horizontal movement NW, and experienced 24.94 mm vertical downward displacement over the observation period (**Figure 2-15**). Above the southern head scarp, KYL-00034 captured 12.00 mm of horizontal movement to W, while dropping in height by 1.44 mm. These small displacement values may be an indication of developing instability upslope of the active headscarp.

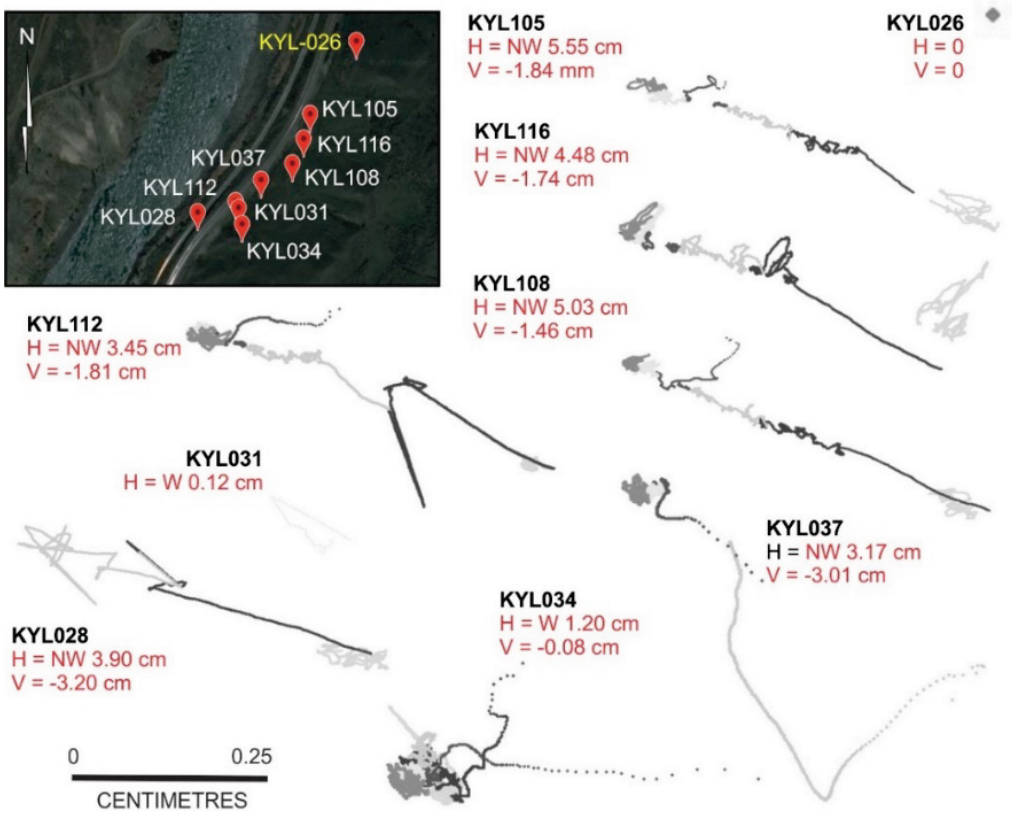

Figure 2-14 Unfiltered displacement trends of Ripley Landslide Geocube™ network. Google Earth image showing active units from December 2018 and provisional results for the November 2018 to June 2019 observation period.

Poor field performance is partly because Geocubes act as a network (i.e., relaying data from one unit to the next until their signals gets to the Geocoordinator. If the network loses a critical nexus (e.g., trains and vegetation blocking signals, or wildlife damaging units), the whole network can slowly come down. Unfortunately, the valley and landslide orientation limited sunlight to the solar panels during the winter (less than 2 hours per day in mid-winter). Given the data uncertainties, limited interpretation of the Geocube plots is possible here. However, the horizontal and vertical displacement values are similar to those measured by the d-GPS monuments, InSAR, and UAV change detection methods. As the Geocube™ network on Ripley Landslide (and South Slide) stabilizes through 2020, data collected (remotely and on-site, respectively) will be processed and presented to graphically show: a) Displacement trends (coloured by month, ArcGIS shapefiles); b) 3D displacement (mm) -vs- Date (month, year); c) Surface angle of movement (angle, degrees) -vs- Date (month, year); d) Precipitation (mm) and 3D displacement (mm) -vs- Date (month, year); and, e) Temperature (° C) and 3D displacement (mm) -vs- Date (month, year).

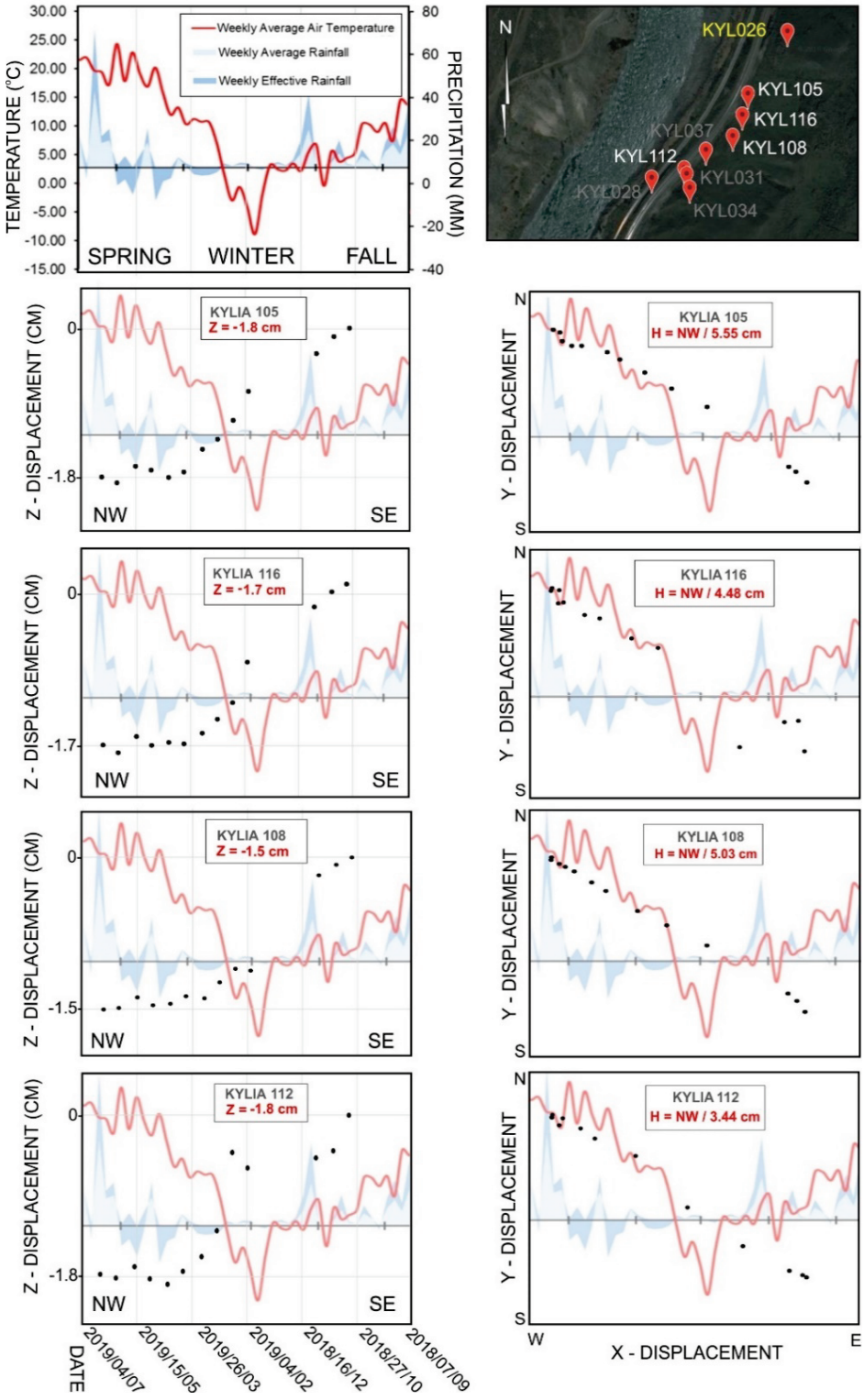

Figure 2-15 Geocube™ displacement results: Z - vertical amounts (cm) and X,Y - horizontal displacements trends for the period September 07, 2018 to June 04, 2019; superimposed are rainfall and temperature data from Thomson Valley weather station (adapted from Holmes et al. 2020, in press). Note that these graphical representations read right to left to represent the displacement trends across Ripley Landslide.

2.3.3.3 Unmanned Aerial Vehicle surveying

UAVs allow flexible, inexpensive acquisition of low-altitude aerial imagery (Bobrowsky et al. 2018). Various off-the-shelf photogrammetric (SfM) software packages enable rapid production of high-quality digital surface models (DSM) from such images. Flying-height and battery restrictions limit the size of such surveys to areas on the order of magnitude of the largest landslides in the Thompson River valley. UAV photogrammetric surveys offer an excellent opportunity to generate high-quality repeat DSMs that can be compared to characterize surface change of active landslides along the transportation corridor. However, wildfires and extremely poor air conditions prevented fulfilment of the flight and survey objectives during the 2017 and 2018 field seasons. With changing climate and weather conditions, poor air quality may limit future sortie times and ranges. In addition, federal aviation regulations are strictly enforced near railway property, requiring personnel with a flying license, and controlled line-of-sight traverses avoiding the railway right-of-way.

Individually, each DSM captures the surface condition of the landslide, including vegetation growth (e.g., grasses, shrubs and trees) that only partly obscure the bare earth. These conditions are sufficient for surface change detection mapping using successive DSMs. Vertical displacement modelling using the SfM show mostly changes in vegetation. Cosi-Corr results (**Figure 2-16**) show >50 cm 3D displacement of blocks along steep-dipping, retrogressive backscarps main slide body from 2016-2018. This high value is consistent with the InSAR and GNSS monument data that captured significant displacement in 2017 (Fig. 3). Displacement along the tracks reflects subsidence of slide body (also expressed in deformation of the lock-block retaining wall), and the addition of ballast during routine safety maintenance. Metre-scale features (e.g., boulders, corner reflectors) are identifiable (**Figure 2-9 b, c**), and horizontal and vertical displacements of, respectively, 20-30 cm and 15 cm have been measured throughout the slide area on the UAV aerial photography (**Figure 2-16**). Over much of the slide body movement is to the NW, except along the northern and southern flanks, where displacement is W. In contrast, channel scour along the slide toe, and submerged bedrock bounding the landslide, drives the body mass generally westward. Zones within the landslide show an average movement of 230 mm between September 2016 and September 2017; areas not expected to show movement (those outside the slide) show an average difference of 1.64 cm, and up to 4.4 cm (within the RMS error of the GNSS and 3D point cloud processing). Measured flow direction of the landslide material is consistently downslope, as would be expected. The absolute position of the rail tracks has moved 12 cm to 27 cm. These datasets now form the basis for ongoing instrumentation of the slide. A zone of high displacement at the south flank of the slide foot is likely the consequence of toe-slope erosion as evidenced by the 15 m-deep scour pool mapped by the bathymetric surveys (**Figure 2-6 a**). Across the much of foot slope however, 3D displacement values show low, reflecting translational movement of the slide mass over sub-horizontal failure planes beneath the tracks and river.

Additional UAV surveys to be conducted from 2020-2025 will extend surface-change characterization of Ripley Landslide and others in the valley (e.g., South Slide and other active landsides). Comparison of these subsequent surveys will allow exceptionally precise quantification of points and rates of movement. These additional surveys will enable comparison of landslide motion over multiple periods, thus providing a further means to evaluate creep acceleration measured by CPR d-GPS monuments, and the GSC d-GNSS markers (Geocubes™).

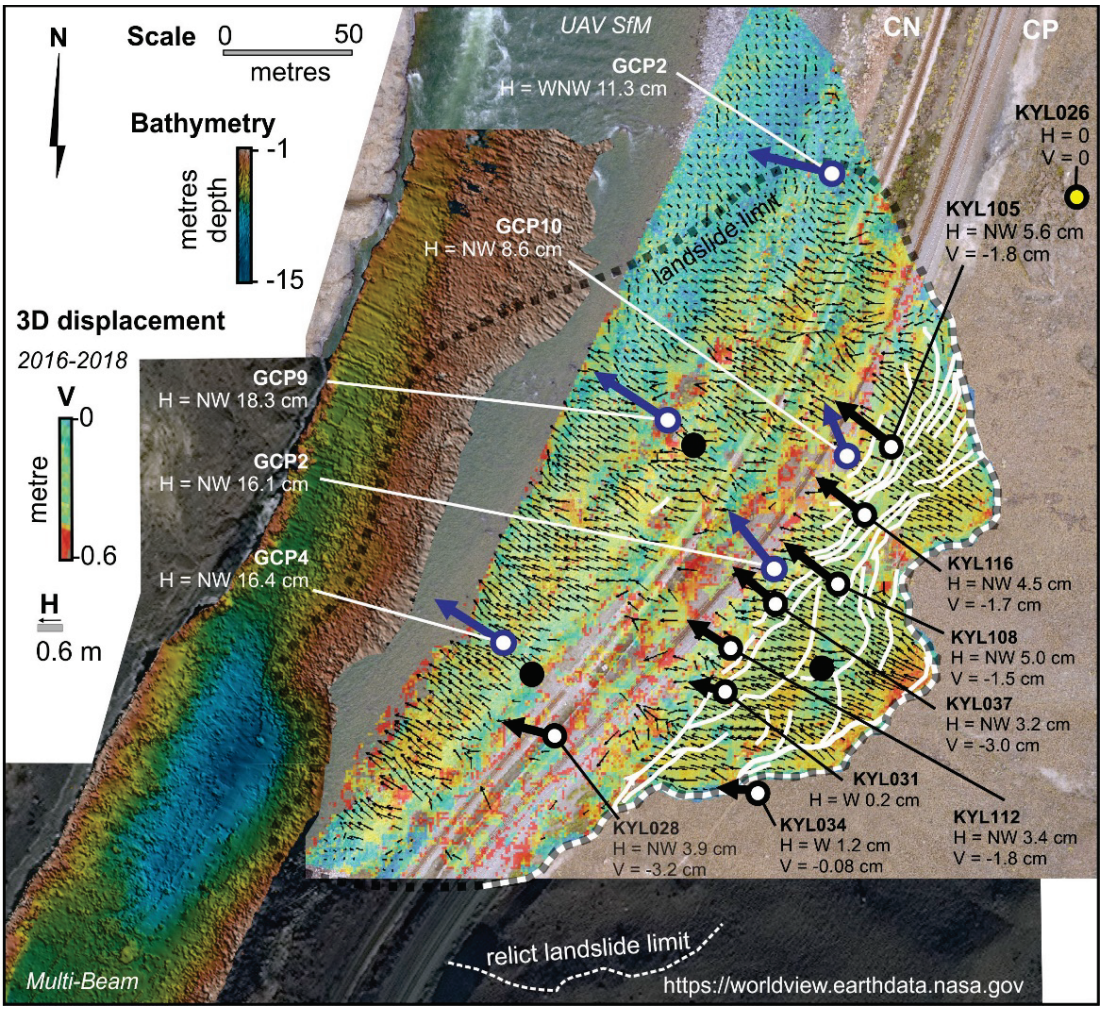

Figure 2-16 Surface displacement data derived from UAV overflights in 2016 and 2018 and multi-beam bathymetry data collected in 2018; plotted with Geocube displacement data (November 2018 to June 2019). Figure also merges multibeam bathymetry data of Thompson River with an outline of Ripley Landslide mapped from a WorldView-2 image of the study site. Stable Geocube – yellow dot; active Geocube – black and white dot; inactive Geocube – black dot. Active GCP – blue and white dot.

2.3.3.4 InSAR change detection

InSAR change detection monitoring using imagery acquired by Canada's RADARSAT-2 has been ongoing since 2013 (Huntley et al. 2017b; Journault et al. 2018). To define magnitudes and spatial-temporal patterns of surface displacement, three ultra-fine microwave beam modes (3 m spatial resolution) are used in the descending orbital node: U5 with an incident angle 34° and azimuth line-of-sight (LoS) of 281°; U16 incident angle 42°, azimuth LoS ≈280°; and U21 with a 45° incident angle and azimuth LoS of 279°. Aluminum trihedral (corner) reflectors were installed at Ripley Landslide for coherent point analysis of persistent scatterer interferograms. Corner reflectors GSC1 and GSC6 rest on stable ground – bedrock and till respectively; GSC2 to GSC5 and GSC7 to GSC9 are installed on unstable terrain (**Figure 2-2**; **Figure 2-11 b, c**). Different viewing geometries allow for the projection of vertical and horizontal displacement (**Table 2-3**).

Table 2-3 Two-dimensional line-of-sight (LoS) displacement rates (cm/yr) for trihedral corner reflectors installed at Ripley Landslide. Values are negative because displacement is westward along the LoS. P1 - August 2013 to April 2014; P2 - May 2014 to August 2014; P3 - September 2014 to April 2015; P4 - May 2015 to August 2015; P5 - September 2015 to April 2016 (adapted from: Huntley et al. 2017b).

InSAR reflector	Vertical (cm/yr)				Horizontal Azimuth 280° (cm/yr)			
	Average	P1	P2-P3	P4-P5	Average	P1	P2-P3	P4-P5
GSC1	0	0	0	-1	0	0	0	0
GSC2	-3.0	-1.8	-0.8	-2.9	-4.1	-11.0	-4.6	-4.3
GSC3	-2.5	-0.9	-0.3	-2.6	-3.7	-11.1	-4.4	-3.5
GSC4	-2.2	-0.6	-0.2	-2.8	-3.2	-10.1	-4.0	-2.8
GSC5	-3.3	-4.9	-0.6	-2.6	-1.8	-5.6	-3.4	-2.1
GSC6	0	0	0	0	0	0	0	0
GSC7	-3.6	-7.8	-0.5	-2.4	-2.9	-5.0	-5.6	-2.9
GSC8	-2.7	-3.1	-0.4	-1.3	-4.7	-12.0	-6.3	-5.1
GSC9	-2.3	-2.7	-1.9	-2.5	-4.7	-16.2	-3.6	-4.5

A network of interferograms was created for SAR acquisitions between fall 2018 and spring 2019 (**Table 2-4**). Several examples were chosen to illustrate the phase change over three discrete intervals, as well as the contributions of various effects such as seasonal changes in coherence (**Figure 2-17**). Wrapped phase measurements start to become visible in the longer interval interferograms which present an integer ambiguity challenge since phase values are only known *modulo* 2π. Highly accurate cumulative deformation and rate measurements cannot be determined from the analysis of single interferograms. It is difficult to distinguish between reliable and unreliable targets, and the statistical redundancy of a multiply interconnected network cannot be leveraged. Qualitative assessment and rough estimates of deformation are still possible. When corrected for all other phase contributions, one fringe cycle $(-\pi , \pi)$ corresponds to $\lambda/2$ or 2.8 cm of line of sight deformation with λ equal to the RADARSAT-2 wavelength of 56 mm. The change in phase over the slide area ranges from nil to approximately 1.6 radians in the 48 days between September 27 2018 and November 14, 2018. Between November 14, 2018 and March 14, 2019 at least one full fringe cycle is visible; however, there is a notable increase in phase noise. This may be associated with both regular temporal decorrelation effects, in addition to seasonal decreases in coherence caused by changes in the surface due to precipitation and ground moisture conditions. The 72 day period between March 14, 2019 and May 25, 2019 also shows a notable change in phase, which is spatially consistent with the slide extents. Spatial coherence of this interferogram is slightly lower than the 48 day pair as expected, and phase values for this period are also wrapped (**Figure 2-17**).

Table 2-4 SAR acquisition intervals for interferograms of Ripley Landslide (see **Figure 2-17**).

Start Date	End Date	Interval
2018/09/27	2018/11/14	48 days
2018/11/14	2019/03/14	120 days
2019/03/14	2019/05/25	72 days

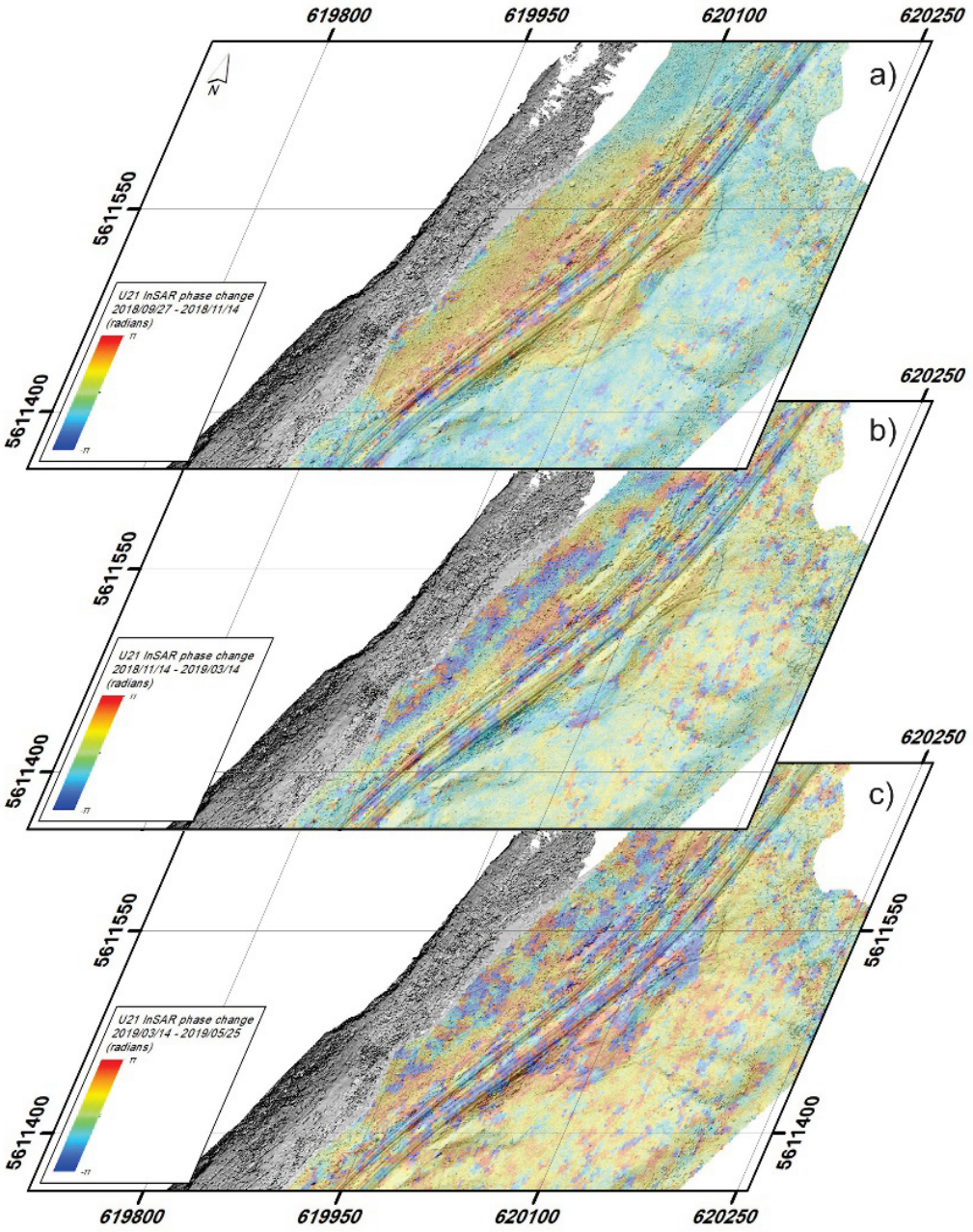

Figure 2-17 Ripley Landslide interferograms for: a) September - November 2018; b) November 2018 - March 2019; c) March 2019 - May 2019.

InSAR results from 2013 to 2015 indicate similar magnitudes and spatial-temporal patterns of displacement as recorded by GNSS and UAV surveys (**Figure 2-18 a**; Huntley et al. 2017b; Journault et al. 2018; Huntley et al. 2020b, in press; Huntley et al. 2020, in review). Ground movement concentrated within the centre of the sliding mass averages 39 mm/year, with fastest displacements detected upslope from the railway tracks, and on the southern flank of the landslide. Average and maximum line of sight (LoS) displacement rates (equivalent to the downslope direction for the west-facing test site) of InSAR corner reflectors and other

coherent targets (e.g., buildings, large boulders) were 49 mm/year, and 77 mm/year, respectively; with greater displacement from November to March (e.g., Huntley et al. 2017b; Journault et al. 2018). Ground movement is concentrated within the main body of the sliding mass and averages 6 cm/year, with fastest displacements detected upslope from the railway tracks (**Table 2-3**).

For Ripley Landslide, a non-linear behavior from May 2014 to April 2016 can be sub-divided into 5 periods. Rates of displacement detected by InSAR vary seasonally, with slower displacement rates occurring during the May to August interval, and higher values from September to April. Peak creep rates observed through winter to spring indicate that river and groundwater levels do not account for all slide movement. Almost no vertical displacement was detected during May to August 2014 (Huntley et al. 2017b; Journault et al. 2018). During the 2016 field season, a climate monitoring station was installed in the Thompson River valley to test whether a component of landslide movement can be attributed to local weather conditions, in particular, precipitation and temperature (**Figure 2-18 b**). In 2017, LoS displacement rate of coherent targets (e.g., corner reflectors, buildings, large boulders), equivalent to the downslope direction for the west-facing test site, was >10 cm/yr (**Figure 2-18 c**). The 18-month climate record (**Figure 2-18 d**) spanning the large displacement event shows that precipitation events were confined mostly between fall and spring, during months when landslide activity increases. This corroborates the results of PRIME monitoring, and indicates fluctuations in temperature over the winter months may contribute to intervals of landslide activity.

Beginning in 2019, and continuing through 2020-2025, RADARSAT-2 results will be compared against data acquired from EUROSPACE platforms (e.g., SENTINEL-1) with different spatial resolutions, view-angle capacities, and orbital paths (**Figure 2-19**). Dedicated processing systems and specific processing algorithms will together reduce processing time and likely improve the quality InSAR results (Pon et al. 2020). The application of advanced processing techniques that consider both persistent scatterer targets and distributed targets (e.g., corner reflectors) will greatly improve the spatial density of displacement records. The main expected outcomes of this activity will be: 1) analysis of the vertical and horizontal deformation components, combining ascending and descending acquisition geometries of satellite data; 2) analysis of the historical datasets and integration with GNSS and UAV data collected *in situ*; 3) improving knowledge of the behaviour and characteristics of the studied landslides; and 4) definition of a sequence of thresholds representative of increasing states of activity of the studied landslides.

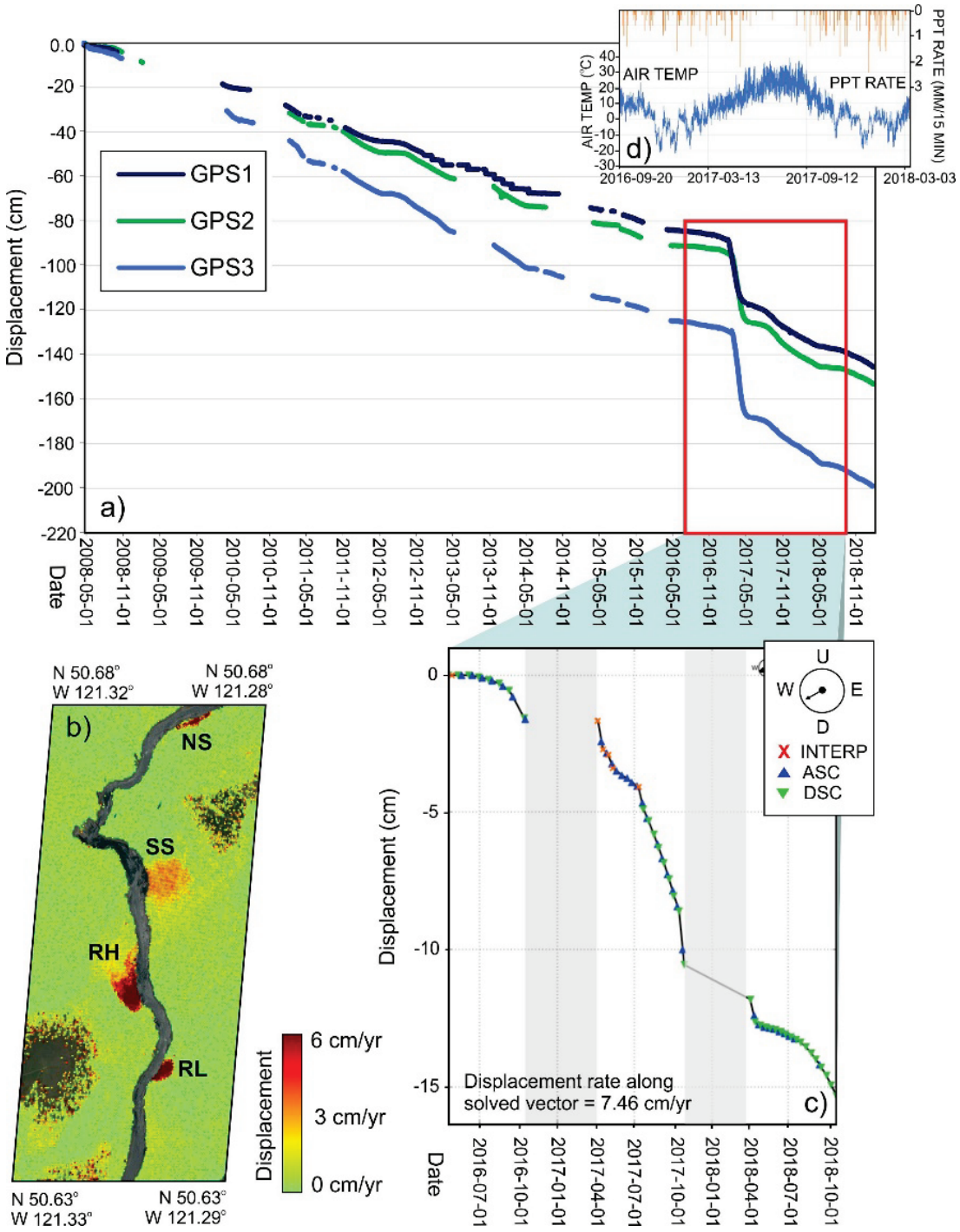

Figure 2-18 Long term change detection monitoring at Ripley Landslide: a, b) InSAR average and 1D LoS displacement rates calculated using temporary coherent targets identified across RADARSAT-2 scenes from July 2016 to October 2018. Multi-master interferograms were created (minus winter scenes, W) with atmospheric effects removed, and signal enhancement including pixel searching and adaptive filtering (Pon et al. 2020). c) Vertical displacement (cm) trackside from May 2008 to January 2019 recorded by GPS1 (-145 cm), GPS2 (-155 cm) and GPS3 (-200 cm); see Fig. 2 for location of GNSS monuments (GNSS data courtesy of D. Wong, CPR). d) Air temperature and precipitation rate recorded at Thompson Valley weather station (**Figure 2-7 b**).

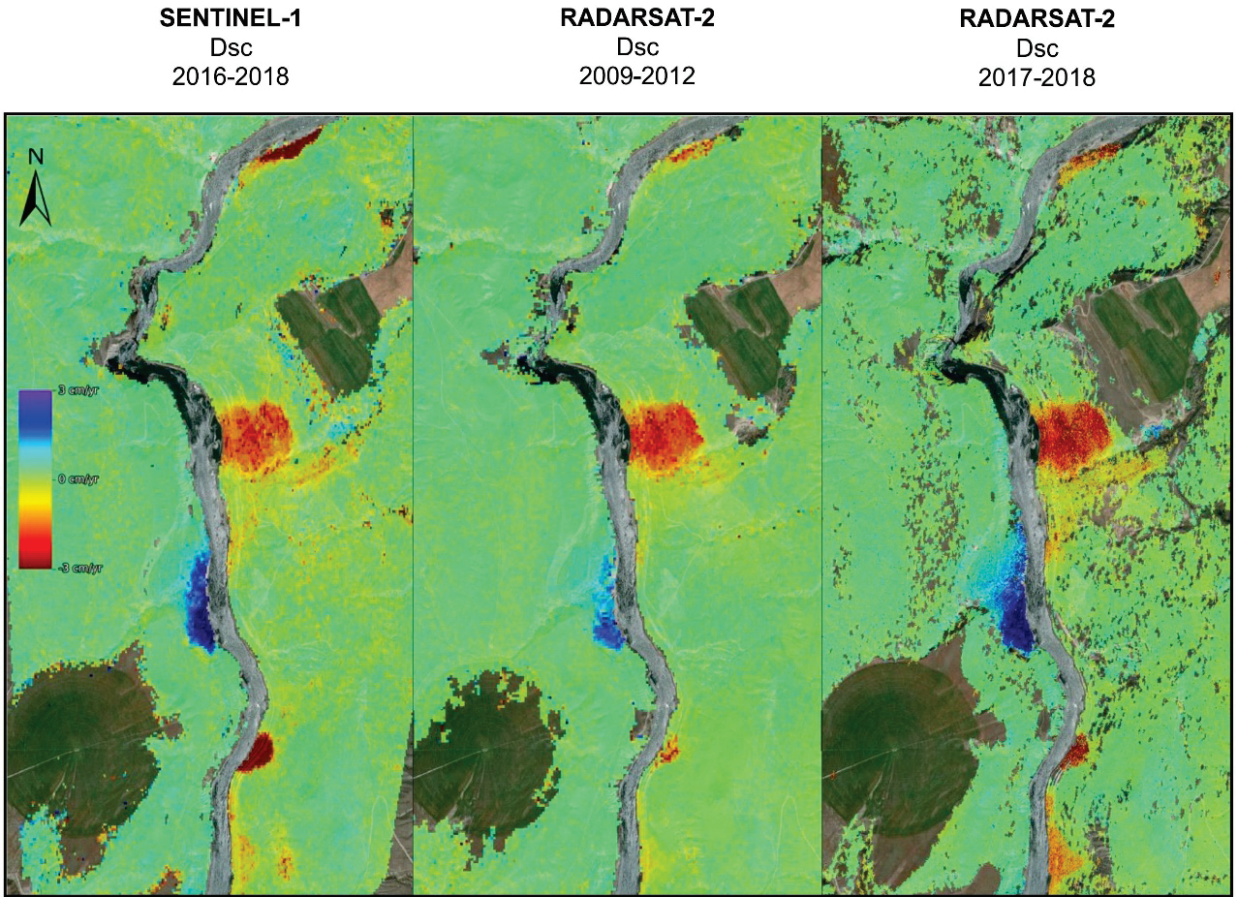

Figure 2-19 Raster comparisons of 1D line-of-sight (LoS) time-series for descending orbits of SENTINEL-1 and RADARSAT-2. Every measurable pixel within this area will have displacement rates assigned. Point coverage for the results (time series) based on displacing areas defined using the signal-to-noise ratio for each pixel (Pon et al. 2020).

3. Conclusions and Implications

3.1 Landslide research and outcomes (2013-2020)

Since 2013, GSC field activities in the Thompson River valley have included: 1) surficial mapping of stable and unstable hillslopes; ground-based, waterborne, and borehole geophysical surveys; 2) installation of 21 InSAR corner reflectors on Ripley Landslide and South Slide; 3) the installation (and decommissioning) of experimental fibre optic systems monitoring strain in a lock-block retaining wall; 4) the installation of a climate station to monitor precipitation and temperature proximal to the studied landslides; 5) installation of experimental Geocube™ networks on Ripley Landslide and South Slide comprising 20 communicating units monitoring temporal and spatial variations in surface displacement; 6) installation of an experimental electrical resistivity system (PRIME) and matric suction sensors at Ripley Landslide that monitors moisture changes in the slope in real-time; and 7) detailed bathymetric mapping of the Thompson River in the vicinity of major slides in the valley to identify zones of erosion and hydraulic connection at submerged landslide toes (**Figure 3-1**; **Table 3-1**).

TC-funded R&D by the GSC and collaborators in the Thompson River valley has: a) comprehensively described the glacial deposits and geophysical characteristics of Ripley Landslide (e.g., Huntley and Bobrowsky 2014; Huntley et al. 2017a, b; Huntley et al. 2020a); b) successfully identified the slope failure mechanism - shear zones in clay-rich beds 5-15 m below the rail tracks (e.g., Hendry et al. 2015; Huntley et al. 2019b,c,d,f); and c) semi-quantified the seasonal fluctuations in Thompson River and groundwater levels in relation to slope instability (e.g., Macciotta et al. 2014; Schafer et al. 2015; Huntley et al. 2016; Holmes et al. 2018; Sattler et al. 2018; Holmes et al. 2019; Holmes et al. 2020). A similar failure mechanism is recognized for other landslides in the Thompson River valley, so the information and knowledge attained from this site can be applied to other sites. InSAR results show that many of the large slides crossed by the CN and CPR tracks are neither relict features or inactive (e.g., Journault et al. 2016, 2018; Huntley et al. 2017c; Journault et al. 2018; Huntley et al. 2020b, in press). These results are helping the railway companies develop effective mitigation and adaptation strategies for the Ripley Landslide, and indicate the need for continued landslide monitoring with complimentary research activities along the rail corridor in the Thormpson River valley (e.g., South Slide, North Slide, Goddard Slide, Barnard Slide, Nepa Crossover, and Red Hill Slide).

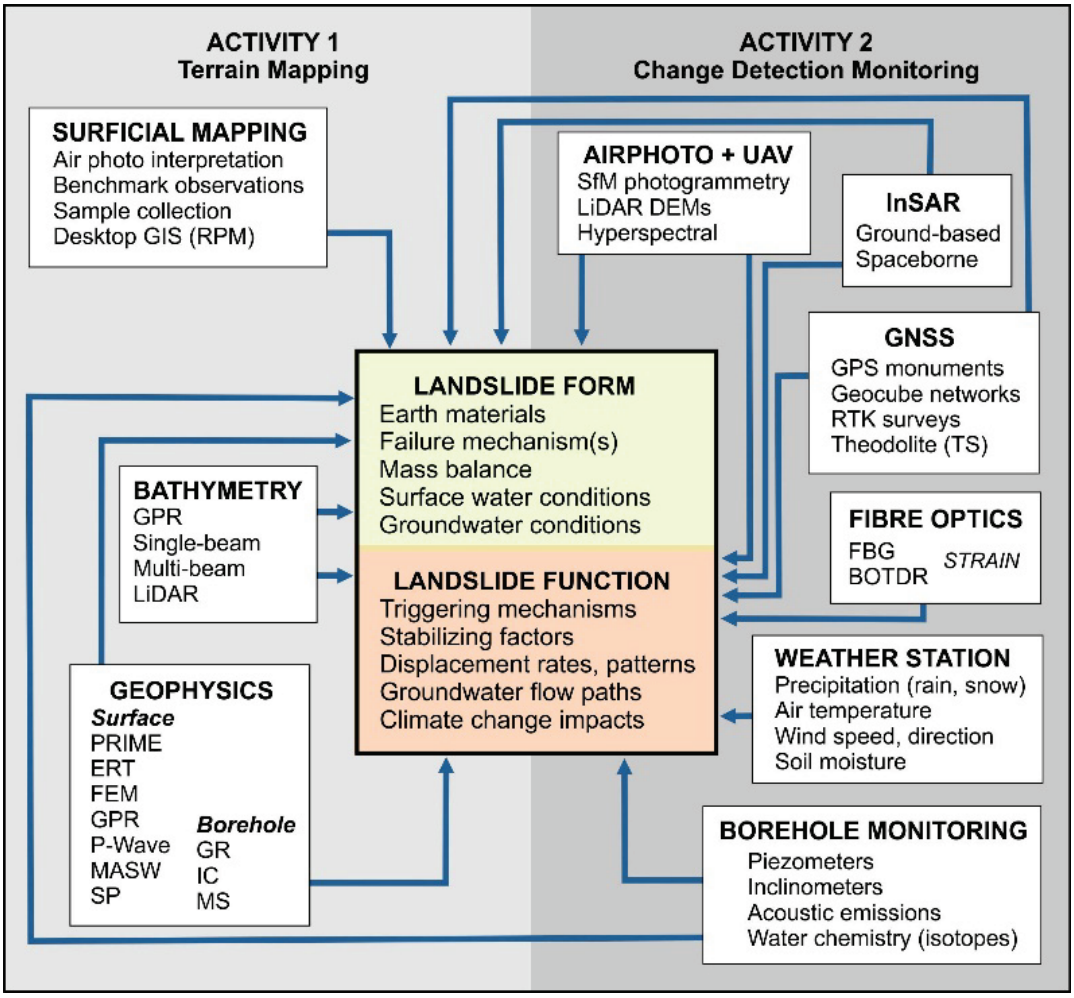

Figure 3-1 Understanding plateau landslide systems through terrain mapping and change detection monitoring based on R&D experience in the Thompson River valley (2013-2020).

Table 3-1 Innovative methods and best practices for ruggedizing monitoring equipment in harsh environments based on experimental successes and failures in the Thompson River valley. Monitoring technologies, operational issues and solutions are discussed in a number of publications and highlighted below in this report (multi-page table).

Monitoring technology	Dates of operation	Environmental and/or technical issues	Solutions
Surface monitoring			
GNSS monuments Macciotta et al. (2014) Hendry et al. (2015)	2010-Present	Monuments easily damaged by heavy rail equipment and passing trains	Lock blocks positioned around track-side monuments for protection Cables buried track-side in protective conduits Computer hardware connected to un-interruptable 12V power supply in CPR signals bungalow
BODTR, FBG fibre optic systems Bobrowsky and Sladen (2013) Bobrowsky et al. (2014b) Bobrowsky et al. (2016) Huntley et al. (2014) Huntley et al. (2016) Huntley et al. (2017d)	2013-2014	Bear damaged fibre optic cables on retaining wall Heavy railway equipment damaged buried cables in conduit Landslide activity damaged buried cables in conduit Computer hardware and instrumentation unreliable at temperatures >30ºC and <-15ºC	Avoid foam-based adhesives when attaching cables to lock-block retaining wall Run fibre optic cables from retaining wall to computer hardware/software in signals bungalow above ground in protective conduit Air conditioning and insulation of hardware in signals bungalow
InSAR corner reflectors Bobrowsky (2013) Bobrowsky et al., (2014a, b, c) Huntley et al. (2017c) Journault et al. (2016) Journault et al. (2018) Huntley et al. (2020b, in prep.)	2013-Present	Deer and cattle use reflectors as rubbing posts Birds use reflectors as perches	Reflectors are repositioned on rebar legs when required Reflectors periodically cleared of bird waste
Geocubes Rodriguez et al. (2018) Holmes et al. (2020)	2018-Present	Deer and rodents chewing through power cables Maintenance of 12V power supply Reliablity of cellular coverage for data telemetry	Power and data cables wrapped in high-impact plastic coil or steel mesh coating Solar panels charge 12V 100AH batteries positioned for maximum insolation Use of omni-directional and directional antennae and service providers (e.g., use of Telus rather than Bell or Rogers)
UAVs Bobrowsky et al. (2017) Bobrowsky et al. (2018) Huntley et al. (2018b) Huntley et al. (2019e)	2016-Present	UAV units are power-heavy Strong mid-afternoon winds funnel up the inner canyon Poor air quality and visibility during summer forest fire season Train operations and schedules influence survey time	Multiple batteries are carried and on charge at the signals bungalow Survey flights restricted to morning hours and early afternoon Surveys flown during fall and spring when fire hazard is low Careful pre-planning of flight-lines to avoid conflicts

Continued over …

Weather station (rain gauge, snow sensor, air temperature) Holmes et al. (2018) Sattler et al. (2018) Huntley et al. (2019c) Huntley et al. (2020a)	2016-Present	Internal electronic component failure of snow sensor prior to installation Maintenance of 12V power supply Reliablity of cellular coverage for data telemetry	Unit repaired, and to be re-installed in 2019 Solar panels charges internal 12V 100AH battery Use of omni-directional and directional antennae and service providers (e.g., use of Telus rather than Bell or Rogers)
Sub-surface monitoring			
Borehole peizometers Macciotta et al. (2014) Hendry et al. (2015) Schafer et al. (2015)	2013-Present	Deer and rodents chewing through power cables Maintenance of 12V power supply Instrumentation sustains damage at shear surfaces	Power and data cables wrapped in high-impact plastic coil Solar panels charge 12V 100AH batteries Careful empacement in borehole with grout and monitor until failure
Borehole inclinometers Macciotta et al. (2014) Schafer et al. (2015)	2013-Present	Deer and rodents chewing through power cables Maintenance of 12V power supply Instrumentation sustains damage at shear surfaces Reliablity of cellular coverage for data telemetry	Power and data cables wrapped in high-impact plastic coil Solar panels charge 12V 100AH batteries Careful empacement in borehole with grout and monitor until failure Use of omni-directional and directional antennae and service providers (e.g., use of Telus rather than Bell or Rogers)
Acoustic emissions sensor (geophone) Bobrowsky et al. (2016) Bobrowsky (2018)	2015-Present	Maintenance of 12V power supply Reliablity of cellular coverage for data telemetry	Solar panels charge 12V 100AH batteries Use of omni-directional and directional antennae
Matric suction sensors Holmes et al. (2018) Sattler et al. (2018) Huntley et al. (2019c) Holmes et al. (2020, in press) Huntley et al. (2020a, in press) Sattler et al. (2020, in review)	2017-Present	Deer and rodents chewing through power cables Reliablity of cellular coverage for data telemetry	Power and data cables wrapped in high-impact plastic coils Use of omni-directional and directional antennae and service providers (e.g., use of Telus rather than Bell or Rogers)

Continued over …

Geophysical monitoring			
ERT-PRIME Parry et al. (2014) Weise et al. (2014) Bauman et al. (2015) Gugins and Candy (2015) Best et al. (2018) Huntley et al. (2017a,b) Theriault and Candy (2017) Holmes et al. (2018) Huntley et al. (2018a) Huntley et al. (2019a, b, c, e, f) Holmes et al. (2020) Huntley et al. (2020a, b, in prep.)	2017-Present	Deer and rodents chewing through ERT cables Reliablity of cellular coverage for data telemetry	ERT cables and electrodes wrapped in rubberized tape, high-density foam, buried to a depth of 50 cm, and covered by cobbles and boulders Use of omni-directional and directional antennae and service providers (e.g., use of Telus rather than Bell or Rogers)
Bathymetric monitoring			
Single-beam acoustic systems Bauman et al. (2015) Young et al. (2017) Huntley et al. (2018b)	2014-2017	Fast-flowing, shallow, turbulent water	Equipment mounted off the stern, on a retractable pole, and protected from jet nozzles when submerged Surveying restricted to reaches without rapids
Multi-beam acoustic systems Huntley et al. (2018b)	2017-2018	Fast-flowing, shallow, turbulent water	Equipment mounted mid-ships, on a retractable pole, and protected below jet hull when submerged Surveying restricted to reaches without rapids

The combination of data from surficial geology mapping, and an array of landslide monitoring and geophysical methods provide significantly more information than any one technique on its own (**Figure 3-1**). This information contributes the physical context for understanding results from other monitoring programs underway (e.g., GNSS, UAV, and InSAR change detection), and will help ensure the safety and security of critical railway transportation infrastructure, thereby reducing risks to public safety, the environment, natural resources, and economy of Canada and globally. Ground deformation detected by monitoring technologies has been minor (in the order of mm to cm), and has not triggered or required significant interventions on behalf of the railways other than routine, but costly, track maintenance. For example, hot wheel detectors were briefly placed on the CN tracks along the retaining wall in 2016. This is where GNSS, InSAR, UAV, and fibre optic monitoring have all detected ground movement. Photogrammetric studies show that from September 2016 to September 2018, small-scale features across the slide body have moved 200-300 mm horizontally and +/- 150 cm vertically. Considering the slower rates of past movement (<50 mm / yr) prior to 2016 recorded by GNSS and InSAR, this increased movement might become a significant risk to railway infrastructure over the coming years. For example, an increased rate of activity may indicate a transition to faster long-term steady creep, or possibly gradual acceleration of the slope that could trigger future rapid failures. Evaluation of future GNSS, InSAR, and UAV change detection results will provide further insight in the processes and possible drivers of this accelerated creep.

3.2 Limitations and Challenges to R&D

The experiences of the 2013-2020 field seasons show that landslide monitoring equipment is often unreliable in the extremely harsh environments of the Thompson River valley. Fibre optic and wire cables have been damaged by deer, rodents and other large mammals. Also routine track maintenance has damaged GNSS instruments and InSAR reflectors. This damage requires innovative and unorthodox methods to protect cables and hardware (**Table 3-1**). Technical issues with experimental systems require frequent software updates, and changes in product designs require re-installation and re-calibration over the coming field seasons (i.e., 2020-2025). Considerable time and effort was spent ruggedizing electronic systems and other hardware against changing environmental conditions in the BC south-central interior. For the years ahead, a significant challenge facing the GSC will be the availability of essential team members. Commitments in other program areas will limit access to the critical NRCAN technical support required to install and maintain the landslide monitoring networks, process data, and interpret results. A solution to this human resource shortage is to encourage university partners to create theses (M.Sc. and Ph.D.) and post-doctoral projects for new students and recent graduates.

3.3 Best practices for future landslide studies (IMOU-5170)

Understanding landslide form and function ultimately reduces geohazard-related socioeconomic risks. The long-term monitoring successes in the harsh environment of the Thompson River valley highlighted in this report suggest a two-pronged approach for future studies in transportation corridors where landslides are a geohazard (**Figure 3-1**). *Terrain Mapping Activities* incorporate surficial geology mapping, bathymetric, and geophysical surveys, with real-time monitoring of movement, groundwater, and geophysical properties in boreholes and on slopes to describe landslides, adjacent stable slopes, and interacting water bodies. *Change Detection Monitoring Activities* describe landslide function using emerging ground-based GNSS systems and weather stations, geophysical arrays in boreholes and on slopes, photogrammetry using unmanned airborne vehicles, and radar interferometry with spaceborne platforms (**Figure 3-1**).

Near-surface geophysics, GNSS, UAV, and InSAR have been shown to be effective at locating portions of the landslide(s) with the highest creep rates. Understanding spatial variability in landslide motion improves landslide characterization and mitigation efforts. For example, determining whether failure involves complex interactions between structurally separate blocks that could preferentially move and damage railway infrastructure. This knowledge will help identify where and track and ballast damage can be expected, allowing railway companies and contractors to plan targeted maintenance, leading to reductions in operational delays and cost savings. Comparing displacement trends with proxy records of possible landslide drivers – including temperature, precipitation, river level and irrigation will help establish landslide warning threshold based on environmental conditions. For example, detailed analyses of GNSS, UAV, and InSAR displacement histories spanning acceleration periods may reveal environmental triggers (e.g., warm/dry intervals or cool/wet intervals in climate data time-series). If gradual acceleration is found to precede rapid displacement events similar to that observed in 2017, future monitoring accelerated creep can be used to forecast impending failures.

The objectives of IMOU-5170 between NRCan-GSC and TC-IC are to: 1) gain a better understanding of how geological conditions, extreme weather events and climate change influence landslide activity in the Thompson River valley, British Columbia, and the Assiniboine River valley, Saskatchewan-Manitoba; 2) develop reliable real-time monitoring solutions for critical railway infrastructure (e.g., ballast, tracks, retaining walls, tunnels and bridges) able to withstand the harsh environmental conditions of Canada; and

3) contribute to more robust risk tolerance, remediation, and mitigation strategies of key stakeholders (i.e., TC-IC, CN and CPR) in order to maintain the resilience and accessibility of critical transportation infrastructure along strategically important sections of the national railway network, while also protecting the natural environment, community stakeholders, and Canadian economy.

4. Acknowledgements

For their geophysical services, we wish to thank Neil Parry, Megan Caston, Cassandra Budd and Gordon Brasnett (EBA-TetraTech, Edmonton, Alberta) in 2013-2014; Paul Bauman, Landon Woods and Kimberly Hume (Advisian, Worley Parsons Group, Calgary, Alberta) in 2014-2015; Cliff Candy, Larry Theriault, Caitlin Gugins and Heather Ainsworth (Frontier Geosciences Inc., North Vancouver, BC) from 2015-2017; and Mel Best (BEMEX Consulting International, Victoria, BC). The PRIME installation (2017 to present) is a collaboration with Helen Reeves and colleagues (British Geological Survey, Nottingham, UK). Fieldwork would not be possible without the support of Trevor Evans (Canadian National Railway, Kamloops, BC), and Danny Wong and Jason Bojey (Canadian Pacific Railway, Calgary, Alberta). This Open File was critically reviewed by Roger C. Paulen (GSC Ottawa).

5. References

Bauman, P., Woods, L. and Hume, K. (2015) 2014 Geophysical Investigation at the Ripley Landslide, Thompson River Valley, South of Ashcroft, B.C. *Worley Parsons Canada*, Unpublished Report for the Geological Survey of Canada, 15 pages

Best, M. Bobrowsky, P. Huntley, D., Macciotta, R. and Hendry, M. (2018) Integrating terrestrial and waterborne ERT surveys at the Ripley Landslide near Ashcroft, British Columbia, Canada. *Environmental and Engineering Geophysical Society, Proceedings Volume of 31st SAGEEP*, Nashville, Tennessee, 1 page

Bobrowsky, P. (2013) Recent advances in landslide monitoring. Paper presented at *CIRiDe-International Congress on Disaster Risk and Sustainable Development*, Catamarca, Argentina, 1 page

Bobrowsky, P. (2016) Ripley Landslide: a Canadian test site for landslide investigation and monitoring. *International Consortium on Landslides*, *Technical Presentation*, ICL Board Meeting, Paris, 1 page

Bobrowsky, P. (2018) IPL-202 Ripley Landslide Monitoring Project (Ashcroft, B.C., Canada). International Programme on Landslides, *Unpublished Annual Report*, 1 page

Bobrowsky, P. and Sladen, W. (2013) Installing Fibre Optics with the China Geological Survey. *NRCAN-ESS S&T Newsletter*, Issue #21 (NRCan Wiki online digital version only)

Bobrowsky, P.T., Sladen, W., Huntley, D., Zhang, Q., Bunce, C., Edwards, T., Hendry, M., Martin, D. and E. Choi (2014) Multi-parameter monitoring of a slow moving landslide: Ripley Slide, British Columbia, Canada. In: Engineering Geology for Society and Territory – Volume 2 Landslide Processes, edited by G. Lollino, D. Giordan, G. Battista Crosta, J. Corominas, R. Azzam, J. Wasowski and N. Sciarra; IAEG (International Association of Engineering Geology and the Environment) Congress, Turin, Italy 15 – 19 September 2014, Springer Publishing (Contribution #20140007), pp. 155-159

Bobrowsky, P., Huntley, D., Hendry, M., Macciotta, R., Martin, D., Elwood, D., Lan, H., Bunce, C., Choi, E. and T. Edwards (2014) Lessons learned from fibre optic monitoring of a landslide. Proceedings Abstract, *Geological Society of America, Proceedings Volume of the Annual Meeting*, Vancouver, British Columbia, Canada, 1 page

Bobrowsky, P., Huntley, D., Zhang, Q., Hendry, M., Martin, D., Macciotta, R., Lan, H., Edwards, T., Bunce, C., and Choi, E. (2014) Instrumental monitoring, terrain mapping and geophysical investigations of an active landslide near Ashcroft, British Columbia: tools to better understand, engineer and manage the risks of railway ground hazards. Proceedings Abstract, *Geological Society of America*, *Proceedings Volume of the Annual Meeting*, Vancouver, British Columbia, Canada, 1 page

Bobrowsky, P.., Huntley, D., Hendry, M., Macciotta, R., Schafer, M., Journault, J. Zhang, Q., Zhang, X. and Lv, Z. (2016) Assessing multi-sensor technologies and methods in monitoring landslide movement in Canada. *35th International Geological Congress*, Abstracts and Proceedings Volume, Cape Town, South Africa, 1 page

Bobrowsky, P., Huntley, D., Neelands, P., MacLeod, R., Mariampillai, D., Hendry, M., Macciotta, R., Reeves, H. and Chambers, J. (2017) Ripley Landslide – Canada's premier landslide field laboratory. *Geological Society of America, Proceedings Volume of the Annual Meeting*, Seattle, Washington, USA, 1 page

Bobrowsky, P., MacLeod, R., Huntley, D., Niemann, O., Hendry, M., Macciotta, R. 2018 Ensuring Resource Safety: Monitoring Critical Infrastructure with UAV Technology. Resources for Future Generations, Conference Abstracts Volume, Vancouver, Canada, 1 page

Bunce C. and Chadwick, I, (2012) GPS monitoring of a landslide for railways. In: Eberhardt E, et al (eds.) Landslides and Engineered Slopes - Protecting Society through Improved Understanding, pp.1373-1379

Clague, J. and Evans, S. 2003. Geologic framework for large historic landslides in Thompson River valley, British Columbia. Environmental and Engineering Geoscience, Vol 9 (3), pp. 201-212

Gugins, C. and Candy, C. (2015) Downhole logging and multi-spectral analysis of surface waves (MASW) investigation, Ripley Landslide Project, Ashcroft area, B.C. *Frontier Geosciences Inc*. Unpublished Report for the Geological Survey of Canada, 20 pages

Hendry, M., Macciotta, R. and Martin, D. (2015) Effect of Thompson River elevation on velocity and instability of Ripley Slide. Canadian Geotechnical Journal, Vol. 52(3), pp. 257-267

Holmes, J., Chambers, J., Donohue, S., Huntley, D., Bobrowsky, P., Meldrum, P. Uhlemann, S., Wilkinson, P. and Swift, R. (2018) The Use of Near Surface Geophysical Methods for Assessing the Condition of Transport Infrastructure. Civil Engineering Research Association, Special Issue on Structural Integrity of Civil Engineering Infrastructure, *Journal of Structural Integrity and Maintenance*, 6 pages

Holmes, J., Donohue, S., Chambers, J., Wilkinson, P., Meldrum, P., Gunn, D., Swift, R., Dashwood, B., Kirkham, M., Uhlemann, S., Huntley, D. and Bobrowsky, P. (2019) Long-term monitoring of slopes that affect transport infrastructure. European Association of Geoscientists and Engineers, 1st Conference on Geophysics for Infrastructure Planning, Monitoring and BIM, The Hague, Netherlands, Abstracts Volume, 1 page

Holmes, J., Chambers, J., Meldrum, P., Wilkinson, B., Williamson, P., Huntley, D., Sattler, K., Elwood., D., Sivakumar, V., Reeves, H. and Donohue, S. (2020) 4-Dimensional Electrical Resistivity Tomography for continuous, near-real time monitoring of a landslide affecting transport infrastructure in British Columbia, Canada. Near Surface Geophysics, 34 pages

Huntley, D. (2015a) Railways and Landslides in the Thompson River valley, British Columbia, Canada. *Geological Survey of Canada*, Geoscience Information Product 109E, 2 pages

Huntley, D. (2015b) Glissements de terrain et chemins de fer dans la vallée de la rivière Thompson, en Colombie-Britannique, Earth Sciences Sector, General Information Product 109F, 2 pages

Huntley, D. and Bobrowsky, P. (2014a) Ripley Landslide Activity Transport Canada Report (2013-2014). Unpublished Report submitted annually as part of IDLA-4755 with Transport Canada, 8 pages

Huntley, D. and Bobrowsky, P. (2014b) Surficial geology and monitoring of the Ripley Slide, near Ashcroft, British Columbia, Canada; *Geological Survey of Canada*, Open File 7531, 21 pages

Huntley, D., Bobrowsky, P., Qing, Z., Sladen, W., Bunce, C., Edwards, T., Hendry, M., Martin, D. and E. Choi (2014) Fibre optic strain monitoring and evaluation of a slow-moving landslide near Ashcroft, British Columbia, Canada. In: *Landslide Science for a Safer Geoenvironment*, edited by K. Sassa, P. Canuti and Y. Yin, Volume 1, Springer Verlag. 3rd World Landslide Forum (ICL-IPL), Beijing, China 2 – 6 June 2014 (GSC Contribution #20150019), pp. 415-422

Huntley, D. and Bobrowsky, P. (2015) NRCAN-GSC Public Safety Program Ripley Landslide (2014-2015). Unpublished Report submitted annually as part of IDLA-4755 with Transport Canada, 10 pages

Huntley, D. and Bobrowsky, P. (2016) Ripley Landslide Activity Transport Canada Report (2015-2016). Unpublished Report submitted annually as part of IDLA with Transport Canada, 28 pages

Huntley, D., Bobrowsky, P.., Zhang, Q., Zhang, X., Lv, Z., Hendry, M., Macciotta, R., Schafer, M., Le Meil, G., Journault, J. and Tappenden, K. (2016) Application of Optical Fibre Sensing Real-Time Monitoring Technology at the Ripley Landslide, near Ashcroft, British Columbia, Canada. *Canadian Geotechnical Society, Proceedings Volume of GeoVancouver2016 Annual Meeting*, 13 pages

Huntley, D. and Bobrowsky, P. (2017) Ripley Landslide Activity Transport Canada Report (2016-2017). Unpublished Report submitted annually as part of IDLA with Transport Canada, 35 pages

Huntley, D., Bobrowsky, P., Parry, N., Bauman, P., Candy, C. and Best, M. (2017a) Ripley Landslide: the geophysical structure of a slow-moving landslide near Ashcroft, British Columbia, Canada. *Geological Survey of Canada*, Open File 8062, 59 pages

Huntley, D., Bobrowsky, P. and Best, M. (2017b) Combining terrestrial and waterborne geophysical surveys to investigate the internal composition and structure of a very slow-moving landslide near Ashcroft, British Columbia, Canada. In*: Landslide Research and Risk Reduction for Advancing Culture and Living with Natural Hazards*, Vol. 2, 4th World Landslide Forum (ICL-IPL), Ljubljana, Slovenia 29- May 2 June 2017, Springer Nature, 15 pages

Huntley, D., Bobrowsky, P., Charbonneau, F., Journault, J. and Hendry, M. (2017c) Innovative landslide change detection monitoring: application of space-borne InSAR techniques in the Thompson River valley, British Columbia, Canada. In: *Landslide Research and Risk Reduction for Advancing Culture and Living with Natural Hazards*, Volume 3, 4th World Landslide Forum (ICL-IPL), Ljubljana, Slovenia 29- May – 2 June 2017, Springer Nature, 13 pages

Huntley, D., Bobrowsky, P., Zhang, Q., Zhang, X. and Lv, Z. (2017d) Fibre Bragg grating and Brillouin optical time domain reflectometry monitoring manual for the Ripley Landslide, near Ashcroft, British Columbia ; *Geological Survey of Canada*, Open File 8258, 66 pages

Huntley, D. and Bobrowsky, P. (2018) Ripley Landslide Activity Transport Canada Report (2017-2018). Unpublished Report submitted annually as part of IDLA with Transport Canada, 40 pages

Huntley, D., Bobrowsky, P., Hendry, M., Macciotta, R., Elwood, D., Sattler, K., Reeves, H., Chambers, J., Meldrum, P. Holmes, J. and Wilkinson, P. (2018a) Using multi-dimensional ERT modelling to provide new insight into the hydrogeological structure of a very slow-moving landslide in glacial sediments, Thompson River valley, British Columbia, Canada. *Geological Society of America Annual Meeting*, Session T65, Abstract Volume, 1 page

Huntley, D., Bobrowsky, P., MacLeod, R. and Roberts, N. (2018b) New insights into form and function of very slow-moving landslides from bathymetric surveys of Thompson River, British Columbia *Geological Society of America Annual Meeting*, Session T53, Abstract Volume, 1 page

Huntley, D., Bobrowsky, P., MacLeod, R., Cocking, R. and Joseph, J. (2019a) Thompson River Valley Landslide Activity Transport Canada Annual Report (2018-2019) and Proposal for New Interdepartmental Letter of Agreement (2019-2025). Unpublished Report submitted annually as part of IDLA with Transport Canada, 65 pages

Huntley, D., Bobrowsky, P., Hendry, M., Macciotta, R. and Best, M. (2019b) Multi-technique geophysical investigation of a very slow-moving landslide near Ashcroft, British Columbia, Canada. *Journal of Environmental and Engineering Geophysics*; Vol. 24 (1) pp. 85-108

Huntley, D., Bobrowsky, P., Hendry, M., Macciotta, R., Elwood, D., Sattler, K., Best, M., Chambers, J., Meldrum, P., Holmes, J. and Wilkinson, P. (2019c) Application of multi-dimensional electrical resistivity tomography datasets to investigate a very slow-moving landslide near Ashcroft, British Columbia, Canada. *Landslides*, DOI 10.1007/s10346-019-01147-1

Huntley, D., Bobrowsky, P., Sattler, K., Elwood, D., Holmes, J., Chambers, J., Meldrum, P. Holmes, J. and Wilkinson, P. Hendry, M. and Macciotta, R. (2019d) PRIME installation in Canada: protecting national railway infrastructure by monitoring moisture in an active landslide near Ashcroft, British Columbia. 32nd *SAGEEP, Environmental and Engineering Geophysical Society*. Proceedings Volume of the Annual Meeting, 1 page, Portland, Oregon, USA; Geological Survey of Canada Open File 8548, 1 poster

Huntley, D., Bobrowsky, P., MacLeod, R., Cocking, R., Joseph, J. and Rotheram-Clarke, D. (2019e) Canadian Geoscience Map: Ripley Landslide, Thompson River valley, British Columbia. Geological Society of America, Annual Meeting, Phoenix, Arizona, Abstracts Volume, 1 page

Huntley, D., Holmes, J., Chambers, J., Donohue, S., Meldrum, P., Wilkinson, Elwood, D., Sattler, C., Hendry, M., Macciotta, R. Bobrowsky, P., Cocking, R., Joseph, J. and Rotheram-Clarke, D. (2019f) New advances in near-surface electrical resistivity tomography: understanding the hydrogeological properties and behaviour of a very slow-moving landslide in the semi-arid Thompson River valley, British Columbia, Canada. Geological Society of America, Annual Meeting, Phoenix, Arizona, Abstracts Volume, 1 page

Huntley, D., Holmes, J., Bobrowsky, P., Chambers, J., Meldrum, P., Wilkinson, P., Donohue, S., Hendry, M., Macciotta, R., Elwood, D. Sattler, K., and Roberts, N. (2020a) Hydrogeological and geophysical properties of the very slow-moving Ripley Landslide, Thompson River valley, British Columbia. Canadian Journal of Earth Sciences, 56 pages

Huntley, D., Bobrowsky, Rotheram-Clarke, D., MacLeod, R., Cocking, R., Joseph, J., Holmes, J., Donohue, S., Chambers, J., Meldrum, P., Wilkinson, P., Hendry, M. and Macciotta, R. (2020b, in prep.) Protecting Canada's railway network using remote sensing technologies. Advances in Remote Sensing for Infrastructure, Springer International Publishing, 26 pages

Johnsen, T.F. and Brennand, T.A. 2004. Late-glacial lakes in the Thompson basin, British Columbia: paleogeography and evolution. Canadian Journal of Earth Sciences, Vol. 41 (11), pp. 1367-1383

Journault, J., Macciotta, R., Hendry, M., Charbonneau, F., Bobrowsky, P., Huntley, D., Bunce, C., and Edwards, T. (2016) Identification and quantification of concentrated movement zones within the Thompson River valley using satellite-borne InSAR. *Canadian Geotechnical Society,* Proceedings Volume of GeoVancouver2016 Annual Meeting, 13 pages

Journault, J. Macciotta, R., Hendry, M., Charbonneau, F., Huntley, D. and Bobrowsky, P. (2018) Measuring displacements of the Thompson River valley landslides, south of Ashcroft, B.C., Canada, using satellite InSAR. *Landslides*. Vol. 15 (4), pp. 621-636, DOI 10.1007/s10346-017-0900-1

Macciotta, R., Hendry, M., Martin, D., Elwood, D, Lan, H., Huntley, D., Bobrowsky, P. , Sladen, W, Bunce C., Choi, E and Edwards, T. (2014) Monitoring of the Ripley Slide in the Thompson River Valley, B.C. *Geohazards 6 Symposium, Proceedings Volume,* Kingston, Ontario, Canada, 12 pages

Parry, N., Caston, M., Budd, C. and Brasnett, G. (2014) Geophysical data collection: Electrical Resistivity Tomography, Fixed Frequency Electromagnetic Induction, Ground Penetrating Radar and Seismic Refraction; Ripley Slide, near Ashcroft, BC. *TetraTech EBA* Unpublished Reports for the Geological Survey of Canada, 150 pages

Port of Vancouver (2018) portvancouver.com 2018, URL last accessed 21-01-2020

Pon, A., Tomaszewicz, A. and Leighton, J. 2020) Monitoring of Thompson River valley BC, Canada. Unpublished Report for the Geological Survey of Canada, 65 pages

Rodriguez, J., Hendry, M., Macciotta, R., Bobrowsky, P. and Huntley, D. 2018. High-frequency displacement data for detailed analysis of the relationship between precipitation and landslide kinematics – the Ripley and 10-Mile Slides. Geo-Edmonton 2018. Canadian Geotechnical Society, Proceedings and Abstract Volume, Edmonton, Alberta, 1 page

Sattler, K., Elwood, D., Hendry, M, Macciotta, R., Huntley, D., Bobrowsky, P. and Meldrum, P. (2018) Real-time monitoring of soil water content and suction in slow-moving landslide. *GeoEdmonton 2018*, Proceedings Paper, 8 pages

Schafer, M., Macciotta, R., Hendry, M., Martin, D., Bobrowsky, P., Huntley, D., Bunce, C. and Edwards, T. (2015) Instrumenting and Monitoring a Slow Moving Landslide. *GeoQuebec 2015* Paper, 7 pages

Stanton, R.B. 1898. The great land-slides on the Canadian Pacific Railway in British Columbia. Proceedings of Civil Engineers, Vol 132 (2), pp. 1–48

Theriault, L. and Candy, C. (2017) Synthesis and 3-D modelling of geophysical data from the Ripley Landslide. *Frontier Geosciences Inc*. Unpublished Report for the Geological Survey of Canada, 20 pages

Weise, L., Huntley, D. and Bobrowsky, P. (2014) Geophysical survey results and implications for an active landslide in the Thompson River valley. *Geological Society of America, Proceedings Volume of the Annual Meeting*, British Columbia, Canada, 1 page

Young, G. and Slater, C. (2017) Bathymetric survey of the Thompson River from Ashcroft to Basque Ranch. *Advisian, Worley Parsons Canada*, Unpublished Report for the Geological Survey of Canada, 60 pages

APPENDIX 1

Mandates for Inter-Departmental Letter of Agreement 4755 (IDLA-4755) and Inter-Departmental Memorandum of Understanding 5170(IMOU-5170)

Geological Survey of Canada Team Members
Dr. David Huntley (Lead Scientist)
Dr. Peter Bobrowsky (Emeritus Scientist)
Mr. Drew Rotheram-Clarke (InSAR, UAV, GNSS, GIS Specialist)
Mr. Roger MacLeod (UAV, Bathymetry, GPS, GIS Specialist)
Mr. Robert Cocking (UAV, GNSS, GIS Specialist)
Mr. Jamel Joseph (GNSS, GIS Specialist)

Introduction

Natural Resources Canada (NRCan) has the mandate to acquire fundamental geoscience knowledge to manage Canadian lands and natural resources and to protect Canadians from related risks. To fulfil this core activity, Geological Survey of Canada (GSC) landslide research and development (R&D) in the Thompson River valley was covered by an extended Interdepartmental Letter of Agreement (IDLA-4755) with the Transport Port Canada Innovation Centre (TC-IC) between 2012 and 2020 (Bobrowsky and Sladen 2013; Bobrowsky et al. 2017). Work carried out under this agreement was a foundational activity of the GSC Public Safety Geoscience Program (**Appendix Table 1-1**).

TC-IC-funded R&D is also a core activity of the Railway Ground Hazard Research Program (RGHRP) (**Appendix Figure 1-1**). Priorities for research are agreed upon each year by the GSC, TC-IC, and the RGHRP technical committee. This R&D ensures that the national railway companies, government agencies, and local communities were better informed to: 1) understand slope instabilities affecting rail transport; 2) generate information for engineered slope stabilization; 3) provide quantitative data to help forecast landslide movement; 3) improve the design, safety and security of Canada's transportation infrastructure; and 4) reduce risks to the national economy, physical environment, natural resources, and public safety that accompany landslide activity in the Thompson River valley, BC. In addition, the program disseminates knowledge to community members through outreach workshops. For example, a workshop in Ashcroft in 2014 enhanced First Nations and public awareness of local landslides, and the range of work conducted by RGHRP partners. Although R&D in the Thompson River valley has greatly improved our understanding of landslide processes, all RGHRP researchers recognize that more work is required to ensure safer railway infrastructure in the Thompson River valley, and in order to apply the lessons learned to rail safety elsewhere across Canada (e.g., the Assiniboine and Qu'Appelle river valleys, Saskatchewan-Manitoba). This is core mandate for IMOU-5170 (2020-2025).

For the 2019-2020 fiscal year (**Appendix Tables 1-2** and **1-3)**, fieldwork, workshops, contracts, and information dissemination of research (publications, papers at conferences) were made possible through TC-IC funding ($200K). In-kind support from UA, CPR and CN was ~$50K from each partner (a conservative estimate similar to past years). TC-IC funding amounting to approximately $1.1 million from 2013-2020 has ensured that NRCan (and GSC) met the obligations of IDLA 4755 (**Appendix 2**).

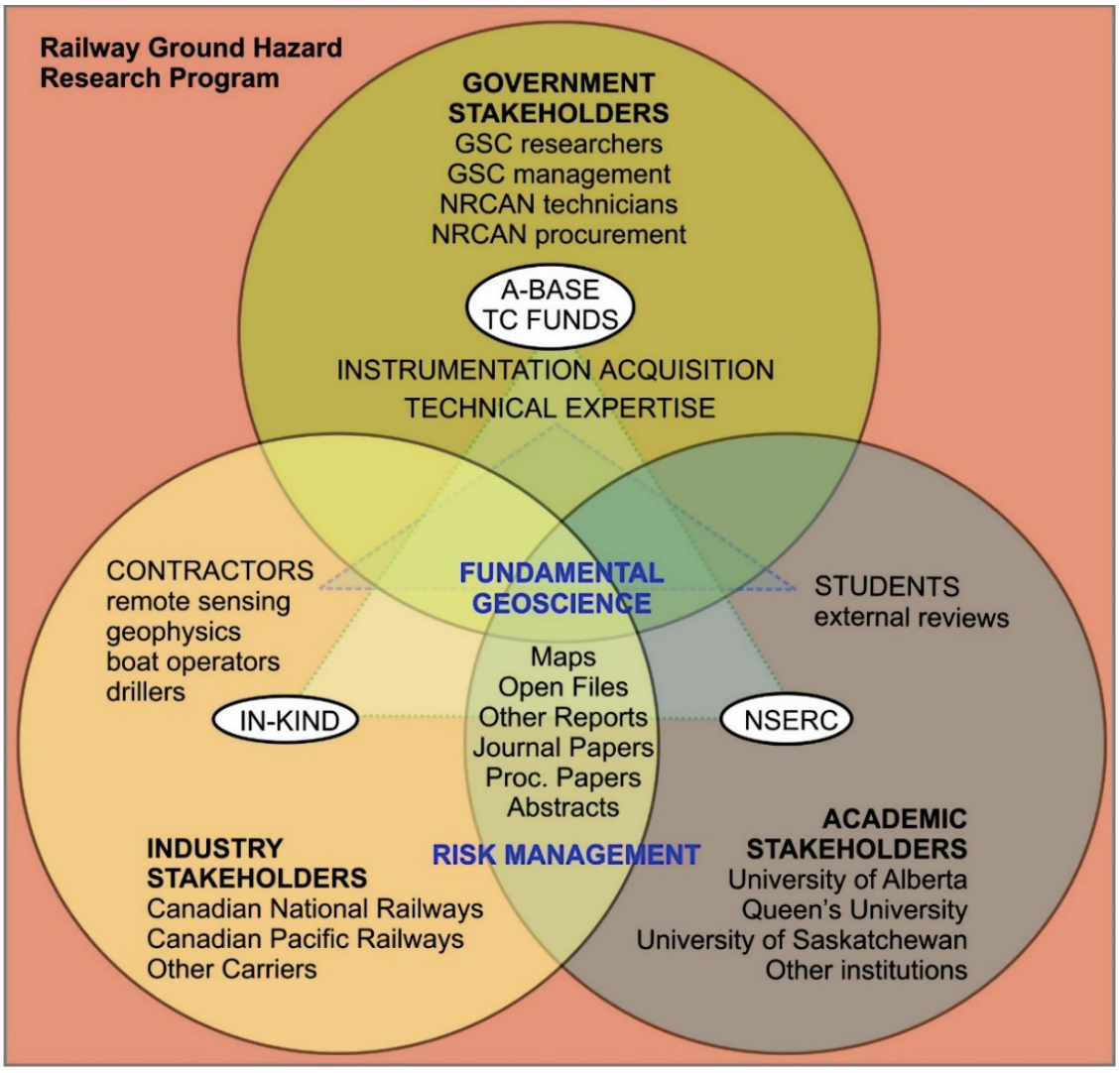

Appendix Figure 1-1 Modified Venn diagram representing the contributions and interactions of key stakeholders in the Railway Ground Hazard Research Program, with funding structure.

Communicating IDLA legacies and international recognition

Research communication activities over the 2013-2020 period included: approximately ninety monthly RGHRP teleconference calls; eight annual RGHRP technical workshops held at venues across Canada; one workshop at the UA Canadian Railway Research Laboratory; two workshops at the CGS Centre for Hydrology and Environmental Geology, Baoding, China; one BGS workshop in London, UK; and a public outreach workshop in Ashcroft, BC. Internal annual reports were also prepared for TC-IC (Huntley and Bobrowsky 2014a; Huntley and Bobrowsky 2015; Huntley and Bobrowsky 2016; Huntley and Bobrowsky 2017; Huntley and Bobrowsky 2018; Huntley et al. 2019a)

Results of geophysical surveys, fibre optical, UAV, and InSAR monitoring were presented at national conferences (e.g., Macciotta et al. 2014; Schafer et al. 2015; Journault et al. 2016; Huntley et al. 2016;),

international fora (e.g., Bobrowsky et al. 2014a,b,c, 2016, 2017; Huntley et al. 2014; Huntley et al. 2017b; Huntley et al. 2018a; Holmes et al. 2019), national and international journals (e.g., Journault et al. 2018; Huntley et al. 2019b, c; Holmes et al. 2020; Huntley et al. 2020a). These GSC and partner-led publications meet NRCan requirements by providing new information in a timely manner to improve the safety and security of Canada's transportation infrastructure, economy, environment, communities, and the public (Huntley et al. 2015a,b,c).

In Ljubljana, Slovenia (May 2017), and in Paris, France (September 2019), the GSC-NRCAN and the UA Department of Civil Engineering were recognized as *World Centres of Excellence in Landslide Research* by the UNESCO International Programme on Landslides (IPL) and the International Consortium on Landslides (ICL). This three-year recognition was awarded based on the collaborative work with TC-IC, CN, CPR and other agencies at Ripley Landslide and Thompson River valley under the RGHRP (Bobrowsky 2016; Bobrowsky et al. 2017). There are only fifteen such recognitions across the globe for landslide excellence. A positive outcome of this recognition and publication record was the interest from other Canadian universities (e.g., USASK), and international institutions (e.g., UNIFI, BGS) to become involved in further collaboration at the Thompson River valley test sites, and elsewhere.

Appendix Table 1-1 Landslide activity partnerships and contributions to the Public Safety Geoscience Program

Government Partnerships	Contributions
China Geological Survey (CGS) Centre for Hydrology, Environment and Geosciences (CGS-CHEGS) *(2010-2015)*	• MOU with CGS for knowledge transfer and to test fibre optic technologies in Canada for measuring deformation of railway infrastructure; in-kind support from CGS amounted to $250K in equipment use and direct spending in the order of $25K • Ripley Landslide was selected as the testbed because on-going RGHRP work provided benchmarking data to test and evaluate fibre optic instrumentation • Real-time monitoring of strain using innovative Fibre Bragg Grating (FBG) and Brillouin Optical Time Domain Reflectometry (BOTDR) systems donated by CGS deployed in Canada • Technical workshops hosted by CGS and GSC in China in 2014 and 2015 • This MOU project ended March 2015
Canada Centre for Mapping and Earth Observation (CCMEO) *(2016-2020)*	• No formal work arrangement • Processing and analyses of InSAR data; collaboration through contributions to conferences, workshops and publications • In-kind support
British Geological Survey (BGS) *(2017-ongoing)*	• In-kind support (~$400K) through sharing PRIME ERT soil-moisture monitoring system, soil moisture monitoring, and publication in the aim of understanding long-term changes in landslide hydrology and impacts on landslide activity
Fisheries and Oceans Canada, Canadian Hydrographic Survey *(2017-2019)*	• No formal work arrangement at present (duration of future support unconfirmed) • Access to single-beam and multi-beam survey equipment (worth $300k), analyses of bathymetric data in proximity to selected landslides; and collaboration in conferences, workshops and publications • In-kind support
Railway Ground Hazards Research Program (RGHRP)	
Transport Canada (TC) *(2012-ongoing)*	• MOU with TC covers GSC participation in the RGHRP monthly teleconferences, workshops and field research • Direct funding for geophysical survey contracts, monitoring instrumentation and extra field work (~$1.1 Million to date) • GSC money provided, and in-kind support from partners was leveraged • A new MOU with TC signed in 2016 • Research activities are scheduled to continue until the end of the new program schedule in March 2020, with TC funding level to be reconfirmed each year.
National Railway Carriers *Canadian National Railways (CN)* *Canadian Pacific Railways (CP)* *(2012, ongoing)*	• In-kind support through hosting teleconferences and workshops • In-kind funding (~$900K) for instrumentation and monitoring • 2013- 2015 drilling costs of $300K covered by the rail companies • Providing rail safety and site access for research scientists
University of Alberta (UA), Department of Civil Engineering *(2012, ongoing)*	• In-kind support (~$600K) through funding for drilling program, instrumentation, field support, monitoring and publication
External Partnerships (Academic and Industry)	
University of Saskatchewan (USASK) Department of Civil and Environmental Engineering (2017, ongoing)	• In-kind support (~$60K) through use of ground moisture instrumentation, terrain change monitoring, and publication • GSC is providing logistical support during matric suction and UAV surveys
University of Victoria (UVIC) Department of Geography *(2017-2019)*	• In-kind support (~$50K) through use of UAV instrumentation ($150k), terrain change monitoring, and publication • GSC is providing logistical support during UAV surveys
University of Florence (UNIFI) Department of Earth Sciences, TRE-Altamira, 3vGeomatics *(2018, ongoing)*	• Remote expertise of 8 3vG, 12 TRE-Altamira, and UNIFI staff members • In-kind support (~$60K) through sharing radar satellite imagery, InSAR processing and monitoring, and publication
Loughborough University, UK *(2016, ongoing)*	• In-kind support (~$50K) through acoustic emission landslide monitoring installation

Appendix Table 1-2 Hydrogeophysics activities matrix 2019-2020

Collaborating Institutions	**Personnel Requirements and Rôles**	**Activity Objectives**	**Preliminary and Projected Outcomes**	**Dissemination (i.e., presentations, publications)**
Geological Survey of Canada	• 2 Research Scientists (Quaternary) • 1 Physical Scientists (Geophysics) • 1 GIS Technician • 1 Postdoc fellow (Training, Continuity)	Maintenance and expansion of PRIME system (possibly to other sites in Canada) Collection and synthesis of data sets Validation of other results Calibration of slope moisture and ground displacement models Geoscience Outreach (conferences, workshops, publications)	**Preliminary:** Characterize the properties and distribution of geologic materials and structures comparison of both subaerial and subaqueous parts of Ripley Landslide *Completed 2020* **Projected (2020-2025):** Characterize the spatio-temporal variability of slope moisture along PRIME system Evaluate possible relationships between soil moisture and landslide activity based on comparison of PRIME results and slope displacement monitoring Develop precipitation and temperature records for the study area Evaluate possible influences of precipitation and ambient temperature on landslide activity based on comparison of meteorological records and slope displacement monitoring Evaluate lag times of soil moisture change behind precipitation events and temperature change based on comparison of meteorological records with PRIME results Evaluate the utility of precipitation, ambient temperature, and soil moisture in predicting landslide activity based on comparison of three-dimensional displacement measurements with PRIME results and meteorological records	**Conferences 2019-2020** EGU2019 GSA2018 SAGEEP2020 IGC2020 (postponed) **Journal Publication** Peer reviewed paper for *Canadian Journal of Earth Sciences* in press GSC senior author Release date 2020 **Government Document** *Open File Report* (GSC) Peer reviewed government report in preparation Release date 2020 **Academic Theses** Student theses *Defence dates TBC* Publications (TBA) BGS, UA and USASK as senior authors
British Geological Survey Queen's University Belfast University College Dublin	• 1 Research Scientist (Geophysics) • 1 Professor • 3 Physical Scientists (Geophysics) • 1 GIS Technician • 1 Ph.D. Student (Geophysics)			
Department of Civil Engineering, University of Alberta College of Engineering, University of Saskatchewan	• 3 Professors / Research Engineers • 2 Ph.D. Students			

Appendix Table 1-3 GNSS-UAV-InSAR activities matrix 2019-2020

Collaborating Institutions	**Personnel Requirements and Rôles**	**Activity Objectives**	**Preliminary and Projected Outcomes**	**Dissemination (i.e., presentations, publications)**
Geological Survey of Canada	• 2 Research Scientists (Quaternary) • 3 Physical Scientist (InSAR, GNSS, Licenced UAV Operator)	Maintenance of Geocube networks on Ripley and South slides Collection and synthesis of Geocube and GNSS data sets Collection and synthesis of UAV and RTK-GNSS data sets Collection and synthesis of InSAR data sets (RS2, RCM, S1, etc.) Validation of other results Calibration of ground displacement models (e.g., InSAR, UAV, LiDAR) Geoscience Outreach (conferences, workshops, publications)	*Completed October 2020* **Preliminary:** Established GNSS networks at Ripley Landslide and South Slide Characterized three-dimensional ground displacement patterns at discrete locations with GNSS UAV and field mapping characterized geomorphology and ground-surface conditions at various times Characterized changes in geomorphology and ground-surface conditions by comparison of sequential UAV surveys Characterized 1-D ground displacement patterns at discrete locations with InSAR at 7 slides **Projected (2020-2025):** Evaluate performance of multi-temporal, UAV-based models against GNSS and InSAR results for characterizing landslide activity Improve characterization of slope activity by combining 3-D GNSS, UAV and InSAR by combining enhanced understanding of landscape morphology from UAV surveys with displacement records (from Geocubes and InSAR), and soil moisture records (from PRIME)	**Conferences 2019-2020** EGU2019 GSA2018 SAGEEP2020 IGC2020 (postponed) **Journal Publication** Peer reviewed paper for *Landslides* in review GSC lead author Release date 2020 or 2021 Peer reviewed paper for *Canadian Journal of Remote Sensing* (or equivalent) in preparation GSC co-author Release date 2020 or 2019 **Government Document** *Open File Report* (GSC) Peer reviewed government reports in preparation Release date 2020 **Academic Theses** Student theses and publications (TBA) UA and USASK senior author Defence date (TBC)
Department of Civil Engineering, University of Alberta	• 3 Professors / Research Engineers • 2 M.Sc./Ph.D. Student			
College of Engineering, University of Saskatchewan				

APPENDIX 2

Research activity goals achieved from 2013-2020

Activity objectives achieved 2013-2015

Work period	Location	Activities	Participants *GSC personnel contributions*
April-May 2013	Ashcroft, BC	Installation of fibre optic systems, InSAR corner reflectors, borehole piezometers, inclinometers	GSC, CGS-CHEGS, CN, CP, UA, TC *2 RES; 2 PC; 1 Emeritus*
July 2013	Ashcroft, BC	Installation of InSAR corner reflectors, terrain mapping	GSC, TC *2 RES, 1 Student*
November 2013	Ashcroft, BC	Terrestrial geophysics survey: ERT, EM, GPR and seismic refraction, terrain mapping	GSC, EBA-Tetratech, TC *1 RES*
December 2013	Montreal, QC	Annual RGHRP workshop: presentation of 2013 results	GSC, TC, CN, CP, UA, other RGHRP members *1 RES*
March 2014	Baoding, PRC	Technical Workshop to address trouble shooting, repair of damage and re-installation of fibre optic systems	CGS, GSC, TC *2 RES*
May 2014	Fredericton, NB	Geological Association of Canada Conference: oral presentation, proceedings abstract	GSC, TC *1 RES*
July 2014	Kingston, ON	Geohazards 6 Symposium: oral presentation, proceedings paper	UA (for GSC)
July-August 2014	Ashcroft, BC	Repair of fibre optic systems, installation of InSAR corner reflectors	GSC, TC, CGS-CHEGS, University of Potsdam, Germany *2 RES, 1 Student*
August 2014	Beijing, PRC	World Landslide Forum: oral presentation, proceedings paper	GSC, TC *2 RES*
September 2014	Turin, Italy	International Association for Engineering Geology Congress: oral presentation, proceedings paper	GSC, TC *1 RES*
October 2014	Vancouver, BC	Geological Society of America Conference: oral and poster presentations, proceedings abstracts	GSC, TC *1 RES*
October 2014	Ashcroft, BC	Waterborne geophysics survey: ERT (part 1)	GSC, TC, Worley Parsons *1 RES*
November 2014	Ashcroft, BC	Waterborne geophysics survey: EM, GPR	GSC, TC, Worley Parsons *1 RES*
December 2014	Edmonton, AB	Annual RGHRP workshop: presentation of 2014 results	GSC, TC, CN, CP, UA, other RGHRP members *1 RES*
February-March 2015	Ashcroft, BC	Drilling program: borehole piezometers, inclinometers	GSC, TC, UA, Geotech Drilling *1 RES*
March 2015	Ashcroft, BC	Borehole geophysics survey: Gamma, Conductivity and MR	GSC, TC, Frontier Geosciences *1 RES*

Activity objectives achieved 2015-2016

Work period	**Location**	**Activities**	**Participants** *GSC personnel contributions*
April 2015	Ashcroft, BC	Installation: piezometers, inclinometers and data loggers	GSC, UA, TC *1 RES*
May 2015	Sidney, BC	ESS Food For Thought Presentation: review and synthesis of results to date	GSC *2 RES*
October 2015	Edmonton, AB	Technical RGHRP workshop: review and synthesis of results to date	GSC, TC, CN, CP, UA *2 RES*
October 2015	Ashcroft, BC	Installation of InSAR corner reflectors on South Slide; preparation for outreach workshop	GSC, TC *2 RES, 1 Student*
October 2015	Baltimore, USA	Geological Society of America Conference: oral and poster presentations, proceedings abstracts	GSC, TC *1 RES*
November 2015	Ashcroft, BC	Waterborne geophysics survey: ERT (part 2)	GSC, TC, Contractor (Worley Parsons) 1 RES
November 2015	Ashcroft, BC	Outreach workshop: town hall-style public lectures at local venue	GSC, TC, CN, CP, UA, other RGHRP members *1 RES*
November 2015	Ashcroft, BC	Decommissioning and removal of >$600K worth of CGS equipment installed at Ripley Landslide and stored at GSC facilities, Vancouver	GSC, TC *1 RES*
December 2015	Baoding, PRC	Return of CHEGS equipment as a GSC obligation in the original MOU with China; combined with technical workshop to discuss results and future opportunities for collaboration	GSC, CGS-CHEGS, TC *2 RES*
December 2015	Vancouver, BC	Acquisition of components for remote weather monitoring station	GSC, TC *1 RES, 1 PC*
March 2016	Vancouver, BC	Acquisition of components for slope change detection monitoring (Geocubes)	GSC, TC *1 RES, 1 PC*

Activity objectives achieved 2016-2017

Work period	Location	Activities	Participants *GSC personnel contributions*
April 2016	Vancouver, BC	Submission of Annual Report Preparing contracts for bathymetry, EM+ERT+GPR surveys and geophysical data reviews	GSC, TC *2 RES*
May 2016	Sidney, BC	Pre-installation testing of Geocubes and weather station components	GSC, TC *2 RES, 1 PC*
June 2016	Ashcroft, BC	Installation of weather station on site	GSC, UA, CP, CN, TC *2 RES, 1 PC*
August 2016	Ashcroft, BC Cape Town, SA	Installation of Geocube system on site Presentation of results at International Geological Congress	GSC, UA, CP, CN, TC *2 RES, 1 PC* GSC, UA, TC *1 RES*
September 2016	Ashcroft, BC Denver, USA	Field testing of weather station and Geocube installations Photogrammetric survey of Thompson River valley slides baseline UAV overflight Presentation of results at Geological Society of America meeting	GSC, UA, CP, CN, TC *2 RES, 2 PC* GSC, UA, TC *1 RES, 1 PC* GSC, UA, TC *1 RES*
October 2016	Vancouver, BC	Presentation of results at GeoVancouver2016	GSC, UA, CP, CN, TC *1 RES*
December 2016	Vancouver, BC	Presentation of results from installations and surveys at RGHRP Annual Workshop	GSC, TC *1 RES*
January 2017	Ashcroft, BC	Geocube installation and testing On-site workshop	 GSC, UA, CP, TC *1 RES, 3 PC*
March 2017	Ashcroft, BC	Geophysical survey: bathymetry Weather station data collection	 GSC, TC, Advisian Worley Parsons *1 RES*
March 2017	Vancouver, BC	Geophysics synthesis: bathymetry and Seismic+ EM+ERT+GPR	GSC, TC, Frontier Geosciences Inc. *1 RES*

Activity objectives achieved in 2017-2018

Work period	Location	Activities	Participants *GSC personnel contributions*
April 2017	Vancouver, BC	Submission of Annual Report	GSC, TC *2 RES*
May 2017	Ashcroft, BC	Installation of Geocube system at Ripley Landslide and South Slide	GSC, UA, CP, CN, TC *1 RES; 3 PC; 3 students*
May 2017	Ljubljana, Slovenia	4th World Landslide Forum Presentation of 2 papers	GSC, UA, TC *2 RES (1 onsite)*
July 2017	Ashcroft, BC	Installation of Geocube system at Ripley Landslide and South Slide	GSC, UA, CP, CN, TC *2 RES; 3 PC*
August 2017	Ashcroft, BC	Installation of Geocube system at Ripley Landslide and South Slide Scoping PRIME installation at Ripley Landslide	GSC, BGS, UA, CP, CN, TC *2 RES; 3 PC*
September 2017	Ashcroft, BC	Installation of Geocube system at Ripley Landslide and South Slide Photogrammetric survey of Thompson River valley slides Trenching and cable laying for PRIME installation at Ripley Landslide	GSC, UA, USASK, UVIC, CP, CN, TC *2 RES; 3 PC; 1 student*
October 2017	Ashcroft, BC Seattle, WA	Installation of Geocube system at Ripley Landslide and South Slide Photogrammetric survey of Thompson River valley slides HydroBall bathymetric survey of Ripley Landslide and South Slide Cable repair for PRIME installation at Ripley Landslide Presentation of results at Geological Society of America meeting	GSC, CHS, UA, CP, CN, TC *3 RES; 3 PC; 1 student* GSC, UA, TC *2 RES*
November 2017	Ashcroft, BC	Installation of Geocube system at Ripley Landslide and South Slide Photogrammetric survey of Thompson River valley slides Multi-beam bathymetric survey of Ripley Landslide and South Slide Cable repair for PRIME installation at Ripley Landslide	GSC, CHS, UA, CP, CN, TC *2 RES; 3 PC; 2 students*
December 2017	Kingston, ON	Presentation of results from installations and surveys at RGHRP Annual Workshop	GSC, TC *2 RES; 3 PC*
January 2017	Ashcroft, BC	Site visit to check on status of equipment and download weather and Geocube data	GSC, TC *1 RES; 1 PC*
March 2017	Ashcroft, BC Nashville, TN	Multi-beam bathymetric survey Presentation of results from geophysical surveys at 31st SAGEEP (Environmental and Engineering Geophysical Society)	GSC, TC *2 RES; 1 PC* GSC, TC *1 RES*

Activity objectives achieved in 2018-2019

Work period	Location	Activity Theme	Activity Task and Outcome	Participants *Collaborators*
April 2018	Vancouver, BC	Summary Document	• Submission of Annual Report	GSC, TC *2 RES*
May 2018	Ashcroft, BC	GNSS Technologies UAV Change Detection	• Installation of Geocube system at Ripley Landslide and South Slide • Photogrammetric survey of Thompson River valley slides	GSC, CP, CN, TC *1 RES; 3 PC*
June 2018	Vancouver, BC	InSAR Change Detection Geophysics	• Resources for Future Generations Conference • Presentation of 2 papers	GSC, UA, TC *2 RES; 1 Postdoc*
August 2018	Ashcroft, BC	GNSS Technologies UAV Change Detection Geophysical Survey Climate variables	• Installation of Geocube system at Ripley Landslide and South Slide • Maintenance of PRIME installation at Ripley Landslide	GSC, BGS, UA, USASK, CP, CN, TC *2 RES; 3 PC; 1 Postdoc*
September 2018	Ashcroft, BC San Francisco, CA	GNSS Technologies Geophysical Survey Climate variables UAV Change Detection Geoscience Outreach	• Installation of Geocube system at Ripley Landslide and South Slide • Photogrammetric survey of Thompson River valley slides • Presentation of results at IAEG	GSC, UA, USASK, UVIC, CP, CN, TC *1 RES; 3 PC; 1 Postdoc* *2 RES; 3 PC; 1 Postdoc*
October 2018	Ashcroft, BC	GNSS Technologies Climate variables UAV Change Detection Bathymetric Change Detection	• Installation of Geocube system at Ripley Landslide and South Slide • Photogrammetric survey of Thompson River valley slides • Cable maintenance for PRIME installation at Ripley Landslide • Multi-beam bathymetric survey of Ripley Landslide (repeat)	GSC, CHS, UA, CP, CN, TC, Boat contractor *1 RES; 3 PC; 1 Postdoc* *2 RES, 2 PC; 1 Postdoc*
November 2018	Indianapolis, IN	Geoscience Outreach	• Presentation of results at GSA	GSC, CHS, UA, CP, CN, TC *2 RES; 3 PC, 1 Postdoc*
December 2017	Calgary, AB	Geoscience Outreach	• Presentation of results from installations and surveys at RGHRP Annual Workshop	GSC, TC *2 RES; 3 PC; 1 Postdoc*
March 2019	Ashcroft, BC Portland, OR	GNSS Technologies Climate variables UAV-Bathymetric Change Detection Geoscience Outreach	• Field site visit for Geocube repair and weather data download • Multi-beam bathymetric survey of Ripley Landslide (repeat) • Presentation, geophysical results at 32nd SAGEEP (Environmental and Engineering Geophysical Society)	GSC, TC, Boat contractor *2 RES; 3 PC*

Activity objectives achieved in 2019-2020

Work period	Location	Activity Theme	Activity Task and Outcome	Participants *Collaborators*
April 2019	London, UK	PRIME technical workshop	• Presentation of PRIME activities at Ripley Landslide and planning for summer fieldwork	GSC, TC *1 RES*
April 2019	Vancouver, BC	Summary Document	• Submission of Annual Report	GSC, TC *2 RES*
June 2019	Ashcroft, BC	PRIME samples GNSS Technologies UAV Change Detection	• Collection and shipping of samples • Maintenance of Geocube system at Ripley Landslide and South Slide • Photogrammetric survey of Thompson River valley slides	GSC, BGS, CP, CN, TC *1 RES; 3 PC*
July 2019	Ashcroft, BC	GNSS Technologies and PRIME array	• Rebooting Geocube and PRIME system	GSC, CP *1 RES*
August 2019	Ashcroft, BC	GNSS Technologies UAV Change Detection Climate variables	• Installation of snow sensor and wind sensors Maintenance of Geocube system at Ripley Landslide and South Slide • Maintenance of PRIME installation at Ripley Landslide	GSC, CP, TC *1 RES; 3 PC*
August 2019	Assiniboine River valley, MB	Site reconnaissance	• Ground inspection at CN and CP landslides	GSC, UA, USASK, CP, CN, TC *1 RES; 2 Ph.D.*
September 2019	Ashcroft, BC	GNSS Technologies Geophysical Survey Climate variables UAV Change Detection	• Installation of Geocube system at Ripley Landslide and South Slide • Photogrammetric survey of Thompson River valley slides	GSC, CP, CN, TC *1 RES; 3 PC*
September 2019	Phoenix, AZ	Geoscience Outreach	• Presentation of results at GSA	GSC, TC *2 RES; 3 PC*
October 2019	Assiniboine River valley, MB	GNSS Technologies Climate variables UAV Change Detection	• RTK survey of GCPs • Photogrammetric survey of Assiniboine River valley slides	GSC, MGS, CP, CN, TC *3 RES; 2 PC*
December 2019	Carleton University Ottawa, ON	Geoscience Outreach	• Presentation of results from installations and surveys at RGHRP Annual Workshop	GSC, TC *2 RES*
March 2020	Ashcroft, BC	GNSS Technologies Climate variables UAV Change Detection	• Maintenance of Geocubes, PRIME, weather station, and cameras	GSC, TC *1 RES*